NTNU – Trondheim
Norwegian University of
Science and Technology

Fuel Optimal Thrust Allocation In Dynamic Positioning

Martin Rindarøy

Master of Science in Engineering Cybernetics (2)
Submission date: May 2013
Supervisor: Tor Arne Johansen, ITK

Norwegian University of Science and Technology
Department of Engineering Cybernetics

Abstract

This thesis gives a short introduction to the Dynamic Positioning (DP) domain and focuses on developing a fuel optimal thrust allocation algorithm for marine DP vessels with a diesel electric power plant. Obtained data is used to develop a static model for the fuel consumption of a diesel generator, as a function of its produced power. This model is used to formulate a convex Quadratic Programming (QP)-problem that finds fuel optimal solutions to the thrust allocation problem. This is possible due to the fact that DP vessels are usually over-actuated in terms of their thrusters. The fuel optimal thrust allocation algorithm shows promising results with respect to minimizing consumed fuel of the generators, when compared to thrust allocation algorithms that minimizes produced thrust or consumed power by the thrusters. The simulations in this thesis typically gives a fuel reduction on a rather common Platform Supply Vessel (PSV) of up to 2% of its maximum possible fuel consumption, when compared to thrust and power minimizing thrust allocation algorithms. The fuel optimization can be implemented as a standard QP-problem by recalculation of its cost function weights based on linear and quadratic model approximations at the current operation point. A method for reducing load variations in the diesel generators produced power, and its implications on fuel consumption, sooting and NO_x emission is proposed and discussed. Additionally, simulations of the thrust allocation assisting the Power Management System (PMS) by reserving power on the bus for external consumers about to connect are presented, and it is shown that it might prevent start-up of extra generators.

Sammendrag

Denne masteroppgaven gir en kort introduksjon til Dynamisk Posisjonering (DP) og har hovedfokuset på utviklingen av en drivstoff optimal thrusterallokeringsalgoritme for maritime DP fartøy med diesel elektrisk kraftverk ombord. Innhentet data ble brukt til utvikling av en statisk modell for drivstofforbruket til en diesel generator, som funksjon av dens generte kraft. Denne statiske modellen blir brukt til å formulere et konvekst QP-problem som finner drivstoff optimale løsninger på thrusterallokeringsproblemet. Dette er mulig på grunn av at DP fartøy som regel er over-aktuert med tanke på thrustere. Den drivstoff optimale thrusterallokeringen gir lovende resultater når den sammenlignes med kjente thrusterallokeringer som er optimale i forhold til produsert thrust eller effekttrekket til thrusterene. Simuleringene i denne masteroppgaven gir en drivstoffreduksjon på et standard PSV fartøy på opptil 2% av maksimum mulig drivstofforbruk, når den drivstoff optimale thrusterallokeringen sammenlignes med thrust- og thruster effekttrekk minimerende thrusterallokeringer. Den fuel minimerende thrusterallokeringen kan implementeres som et standard QP-problem ved rekalkulering av kostfunksjonsvekter basert på lineære og kvadratiske model approksimasjoner rundt det nåværende operasjonspunktet. En metode for å redusere last variasjoner i diesel generatorenes produserte effekt, og dens implikasjoner på drivstofforbruk, soting og NO_x utslipp er presentert og diskutert. I tillegg er det vist simuleringer av at thrusterallokeringen hjelper PMS ved å reservere last på en av tavlene for utstyr som skal til å kobles til. Det er vist at dette kan hindre oppstart av flere generatorer.

Preface

This report concludes my MSc thesis in Engineering Cybernetics at the Norwegian University of Science and Technology. This project was carried out from January 2013 to June 2013.

I would like to thank my supervisor, Prof. Tor Arne Johansen at the Center for Autonomous Marine Operations and Systems, Norwegian University of Science and Technology for his good advice and guidance during my MSc thesis.

Trondheim, Norway
June 2013

Martin Rindarøy

Contents

CHAPTER 1

Introduction

In today's marine industry there are many operations such as pipelay operations, dredging, crane barge operations, station keeping, drilling, anchor handling etc, that are performed at low speeds and requires the vessel to maintain heading and/or position. In order to achieve this the vessel is equipped with thrusters such that longitudinal and latitudinal thrust forces can be produced at all times, and a DP system to control them. Depending on the vessels operation, and classification society, the requirements for redundancy in the technical design of the thruster-/generator-/busbar-layout can vary. For DP-class 0 and 1 vessels there are no redundancy requirements, so in the case of a single point of failure, position and heading may be lost. DP-class 2 and 3 vessels have redundancy requirements in the technical design of the vessel which states that in the case of a single point of failure, heading and position should not be lost. This usually means that DP-class 2 and 3 vessels are over-actuated such that it can lose half of its thrusters and still maintain position and heading. The vessel must also be redundant in the number of busbars and generators on board, such that it can lose one busbar or half of its generators without loss of heading and position.

The three main parts of a DP control system is a state estimator, high-level motion controller and the thrust allocation algorithm. The state estimator estimates unmeasured states like current forces on the vessel. The high-level

motion controller calculates forces in surge, sway and yaw moment needed to maintain position and heading, while the thrust allocation algorithm takes the vector containing these forces, and calculates thrust magnitude and direction for each active thruster. The thrust allocation algorithm is the focus of this thesis, and it is assumed that if the thrust allocation algorithm manages to generate the desired thrust vector from the DP-controller, position and heading will be maintained. Because of this, vessel dynamics will not be considered in this thesis in order to keep things focused on the issue at hand, namely the thrust allocation algorithm.

The thrust allocation problem, because most DP vessels are usually over-actuated, is usually solved as an optimization problem, searching for solutions within the thrusters physical limitations, while minimizing some user-defined criterion. Thrust allocation has been an active area of research for the past two decades, and the criteria which is minimized are usually produced thrust or consumed power by the thrusters, while taking physical constraints like azimuth turn rate, forbidden zones, maximum thrust capacity etc. into account.

[Bodson, 2002] discusses control allocation in general, but is drawn to flight-control systems. He compares simple unconstrained allocation problems, with the more complex constrained optimization problem and concludes that constrained optimization problems can realistically be considered for real-time control allocation in flight-control systems. Flight control has similarities with marine vessels, so his conclusion can realistically be translated to marine vessels. This conclusion motivates us to engage in formulating the thrust allocation problem as a constrained optimization problem. Another paper which also has a general view of the control allocation problem is [Johansen and Fossen, 2013]. They present both constrained and unconstrained optimization problems to solve the allocation problem, and the criterion to be minimized is usually some penalty related to the use of actuators and/or violation of constraints.

[Fossen and Johansen, 2006] is a survey of control allocation methods for marine vessels. They introduce optimization problems which solves the thrust allocation problem with respect to physical constraints on the thrusters and a constraint which specifies that the DP-command should be obtained. The criterion which is minimized, are slack variables on the DP-command constraint, since there might be situations where it is just not possible to obtain it, and with a hard constraint in these situations the optimization problem would have no feasible solution. In addition to the slack variables, there are different criteria which also includes either the produced thrust, or the consumed power by the thrusters. These criteria are almost used exclusively throughout the literature that concerns thrust allocation for marine vessels. Singularity avoidance, which

is explained more in detail in [Johansen et al., 2004] they solve the optimization problem using Sequential Quadratic Programming (SQP) algorithms. One of the first to mention singularity avoidance in the thrust allocation algorithm is thought to be [Sørdalen, 1997]. In the papers that discuss singularity avoidance, they add a term in the objective function which puts a penalty on the thrust allocation finding solutions that are close to singular. In this context a singular solution means a thruster configuration where you can not produce generalized forces in every direction in the next few time-steps because of rate limitations on the thrusters. An example of this is a configuration where all thrusters produce thrust in the surge direction only. If the DP-command in the next time-step commands forces in sway only, this can not be achieved in the next few time-steps because of the current thruster configuration and their rate limits. In addition to penalising singular configurations, they also relate a cost to produced thrust, or consumed power by the thrusters. [Ruth, 2008] and [Larsen, 2012] also discusses singularity avoidance. Singularity avoidance will not be implemented in the optimization problems formulated in this thesis in order to keep focus on the goal of minimizing fuel consumption of the generators, however, including the singularity avoidance are fairly straightforward.

Thrust allocation algorithms that seek to minimize consumed power of the thrusters are seen throughout the literature, e.g [Jenssen and Realfsen, 2006], [Leavitt, 2008], [Larsen, 2012], [Wit, 2009], [Ruth, 2008], [Veksler et al., 2012b], [Johansen et al., 2004] and [Veksler et al., 2012a].

In [Wit, 2009] quadratic programming and the Lagrange multiplier method are put up against each other to see which one is best suited for thrust allocation. The optimization problems that are formulated seeks to minimize the total use of thrust while making sure the DP-command is obtained. Forbidden zones, turn rate, maximum thrust capacity and rudders are also considered. It was concluded that quadratic programming gave the best results. This motivates us further to formulate the thrust allocation problem as a QP-problem.

[Larsen, 2012] and [Ruth, 2008] formulate optimization problems that seek to minimize power consumption by the thruster. They use a quadratic approximation of the non-linear relationship between a thrusters produced thrust and its consumed power. This makes it possible to formulate a QP-problem that minimizes consumed power by the thrusters. They also discuss sector constraints on thrusters. Sector constraints states that thrusters have certain directions in which they are not allowed to produce thrust. This can be because of several reasons like flushing of other thrusters, divers, ROVs etc. These forbidden zones leads to non-convex thrust regions which means the problem as a whole can not be formulated as a single QP-problem. They solve this

by dividing the non-convex region into several convex sectors and including a supervisory controller which solves each convex sub-problem as a QP-problem, and decides which sub-problem should be used based on some parameters like cost reduction and time between previous switch. Using a quadratic approximation of the non-linear relationship between thrust and consumed power, are also used in [Johansen et al., 2004].

Non-convex thrust regions also appear when a vessel with rudders use them in DP-operations. This is discussed in [Lindegaard and Fossen, 2003] and [Johansen et al., 2003]. The non-convex thrust regions arise because when the propellers give negative thrust, the rudders have no significant effect. Convexification techniques and multi-parametric quadratic programs are used to formulate convex QP-problems which can be solved efficiently. Computation time and numerical reliability are also discussed in [Johansen et al., 2003]. Computation time and numerical reliability of the thrust allocation algorithms presented in this thesis will not be discussed.

A thrust allocation algorithm that assists the PMS are presented in [Veksler et al., 2012a] and [Veksler et al., 2012b]. They introduce a term in the cost function of the optimization problem, that puts a cost on variations in the load on the bus. They also allow small deviations from the DP-command, and use a feedforward signal to the governor on the diesel engines. Thruster biasing in order to assist the PMS with Fast Load Reduction (FLR) is also used. They show that by including this, the load- and frequency variation on the bus will be significantly reduced. Reduction of load variations on the bus will also be discussed in this thesis.

Two methods for reducing frequency and voltage variations in the power distribution system of dynamically positioned vessels are presented in [Mathiesen et al., 2012]. Method number one is called Dynamic Load Prediction (DLP) and it uses predicted future load changes as feedforward to the diesel generators. Method number two is called Dynamic Load Control (DLC) and uses the fact that by accepting small deviations in station-keeping control one can achieve better load control. Part of their motivation for doing this is both reducing frequency- and load variations as well as reducing the number of online diesel generators, where the latter will reduce NO_x emissions, sooting, fuel consumption and maintenance of the engines. They conclude that by using DLP and DLC, frequency and voltage variations can be reduced such that the number of online diesel generators can be lowered without the risk of blackout. finally they mention that DLP is relevant for all types of vessels whereas DLC is mostly relevant for DP vessels experiencing cyclic load variations.

In [Realfsen, 2009] they discuss power usage, NO_x reduction and ideal work-

ing conditions for diesel generators when the DP vessel operates in calm weather. A thrust allocation method where the load is shared on the switchboards in order to bring generators above the catalyst limit without using extra thrust such as thruster biasing, is presented. They show that the method leads to reduced emission of NO_x. Their simulations show that using a thrust allocation method that increases the load on one switchboard, will lead to a significant reduction of NO_x with only a small increase in fuel consumption.

So far the author has not found anything in the literature where the thrust allocation algorithm explicitly includes the fuel consumption of online generators in the cost function. The thrust allocation algorithms in the literature usually minimizes the power consumed by the thrusters and some take the load conditions on the bus into considerations. [Radan, 2008] and [Hansen, 2000], discusses fuel-optimal operation conditions of a diesel generator plant on a vessel, but they both discuss it from a PMS point of view. [Aithal, 2010], [Widd, 2012] and [Guzzella and Onder, 2010] to name a few discuss diesel engines fuel consumption and emissions. The diesel generator models presented in [Aithal, 2010] and [Widd, 2012] seem however to complex to use in a thrust allocation algorithm.

This thesis will investigate the possibility to use the thrust allocation algorithm, in such a way that the fuel consumption of the online generators will be minimized. A simple model for the fuel consumption of a diesel generator as a function of its produced power will be derived from sampled data, and incorporated in an optimization problem which will be used to solve the thrust allocation problem. The fuel consumption of the online generators will be formulated as a quadratic function of thrusters produced thrust and minimized, while making sure that the thrusters operate within their physical limitations and that the DP-command is obtained if possible. A thrust allocation that reduces variations in the generators produced power is also presented. The implications of variations in produced power, on a generators fuel consumption, sooting and NO_x emission is also discussed. A method which can prevent start up of extra generators, by reserving power for external consumers about to connect will be shown. And finally, simulations showing that the thrust allocation algorithm handles single point of failure and worst-case single point of failure will be presented. The simulations in this thesis are illustrated with the DP class 2 PSV Bourbon Tampen.

CHAPTER 2

DP Introduction

A seagoing vessel is subjected to forces from wind, waves and current as well as from forces generated by the propulsion system.
The vessels response to these forces, i.e its change in position, heading and speed, is measured by the position reference systems, the gyrocompass and the vertical reference sensors. Reference systems readings are corrected for roll and pitch using readings from the vertical reference sensors. Wind speed and direction are measured by the wind sensors.

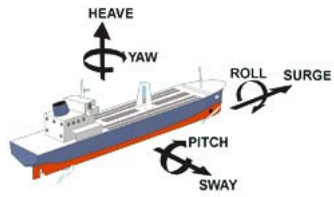

The computer program contains a mathematical model of the vessel that includes information pertaining to the wind and current drag of the vessel and the location of the thrusters. This knowledge, combined with the sensor information, allows the computer to calculate the required steering angle and thruster output for each thruster. This allows operations at sea where mooring or anchoring is not feasible due to deep water, congestion on the sea bottom

(pipelines, templates) or other problems.

Dynamic positioning may either be absolute in that the position is locked to a fixed point over the seabed, or relative to a moving object like another ship or an underwater vehicle. One may also position the ship at a favourable angle towards wind, waves and current, called weathervaning. [Kongsberg, 2012] [Wikipedia, 2012].

[Ådnanes, 2003] and [Fossen, 2002] are both good sources of information on everything that will be superficially presented in this chapter.

2.1 Thruster system

For a vessel to maintain both its position and heading, it needs to be equipped with a thruster system that can provide both transverse and longitudinal thrust. In general, three main types of thrusters are used; main propellers, tunnel thrusters and azimuth thrusters. Main propellers, either single or twin screw are used to create longitudinal thrust, but can in combination with rudders provide transverse thrust as well. For main propellers one can install azipull propellers, which can provide thrust in any direction and does not make use of rudders. Since the main propellers should mainly be used to create longitudinal thrust, the vessel must have well-positioned thrusters to create transverse thrust.

Typically, a vessel will have 2-3 thrusters in the bow and 2-3 thrusters aft, generating thrust both longitudinal and transverse. One of the thrusters in the bow is often chosen to be an azimuth thruster because it provides the opportunity to change the direction of the thrust, while the rest of the thrusters apart from the main propellers are tunnel thrusters.

2.1.1 Thrusters

Thrusters is part of the propulsion system on a ship. Thrusters are mainly used when there is a need for fine manoeuvring of the vessel at low speeds.

There are different kinds of thrusters. Tunnel thrusters is a propeller which is mounted inside the hull and can provide thrust in transverse direction only. An azimuth thruster is inside a closed compartment in the hull when not in use. When the azimuth thruster is needed for manoeuvring it can be lowered from the hull and rotate 360 degrees to provide thrust in all directions in the surge/sway plane. Some thrusters are rpm controlled, whilst others keeps the rpm constant and controls propeller blade pitch instead. Some even combine

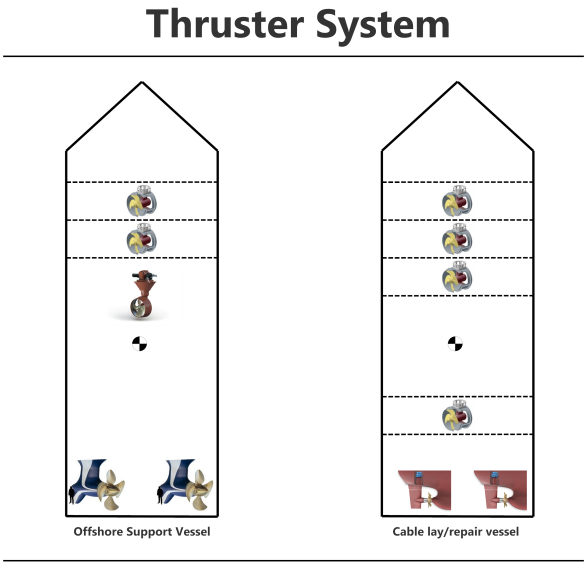

Figure 2.1: Typical thruster layout of two different types of vessels

Azimuth Thruster

Tunnel Thruster

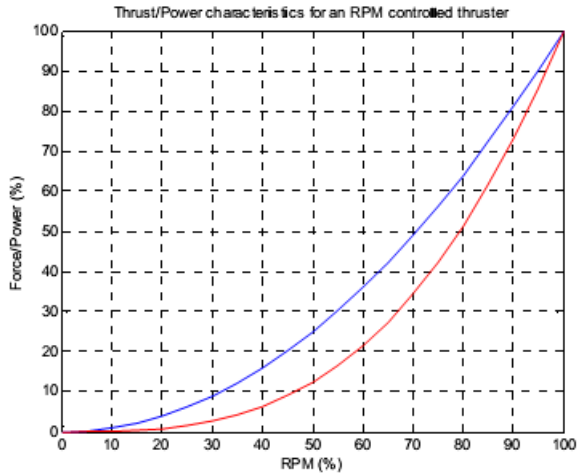

Figure 2.2: Figure showing the Thrust production(Blue) and Power consumption(Red) of an RPM controlled thruster

rpm and pitch control. The effectiveness of a thruster with respect to pitch and rpm is not linear, and follow a combination curve. The combination curve describes how much thrust a thruster gives in tonnes, with a given rpm and pitch. In figure 2.2 which is taken from [Realfsen, 2009], we see how the thrust production and power consumption changes with RPM. In [Realfsen, 2009] they also state that thrust production and power consumption changes with RPM by equation (2.1a) and (2.1b)

$$T = T_0 n^2 \tag{2.1a}$$

$$P = P_0 n^3 \tag{2.1b}$$

where n is the normalized rpm, T_0 is the maximum available thrust and P_0 is the maximum consumed power.

There exists both electrical and diesel driven thrusters, but the most common today is electrically driven thrusters. From [Fossen, 2002] it is found that the relationship between produced thrust and consumed power is given by (2.2)

$$P = |T|^{3/2} \tag{2.2}$$

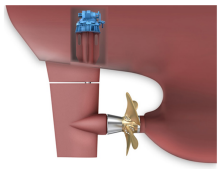

Diesel driven main propulsion

Electrically driven azipull

2.1.2 Main propellers

The main propulsion systems main task is to generate longitudinal thrust. It is used when the vessel is in high speed transit from one location to the other, but can also be used in low speed applications like DP operations.

Main propulsion systems can be both diesel driven, and electrically driven. The diesel driven main propulsion systems has a diesel engine that drives a shaft which usually is connected to a gearbox. From the gearbox a new shaft goes to the aft of the vessel and through the hull to the propellers. With this set-up the propellers can only provide thrust longitudinally. For the vessel to be able to turn it needs rudders as well. The use of rudders in the thrust allocation presents some interesting challenges because of the non-convexity that arises in the available thrust region, because the rudders can only be used to change the direction of thrust when the main propellers exert force in their direction. This is discussed in [Johansen et al., 2003].

Electrically driven main propulsion is done with azipull thrusters. Azipull thrusters can be rotated 360 degrees, but cannot be retracted into the hull like the azimuth thruster [Ådnanes, 2003]. By using azipull thrusters as main propulsion, the vessel will not have large rotating shafts stretching through the vessel. However, it still needs diesel generators to generate power. Since the azipull thrusters can rotate 360 degrees the need for rudders disappear.

2.2 Power system

Central to the operation of any DP vessel are the power generation, supply and distribution systems. Power needs to be supplied to the thrusters and all

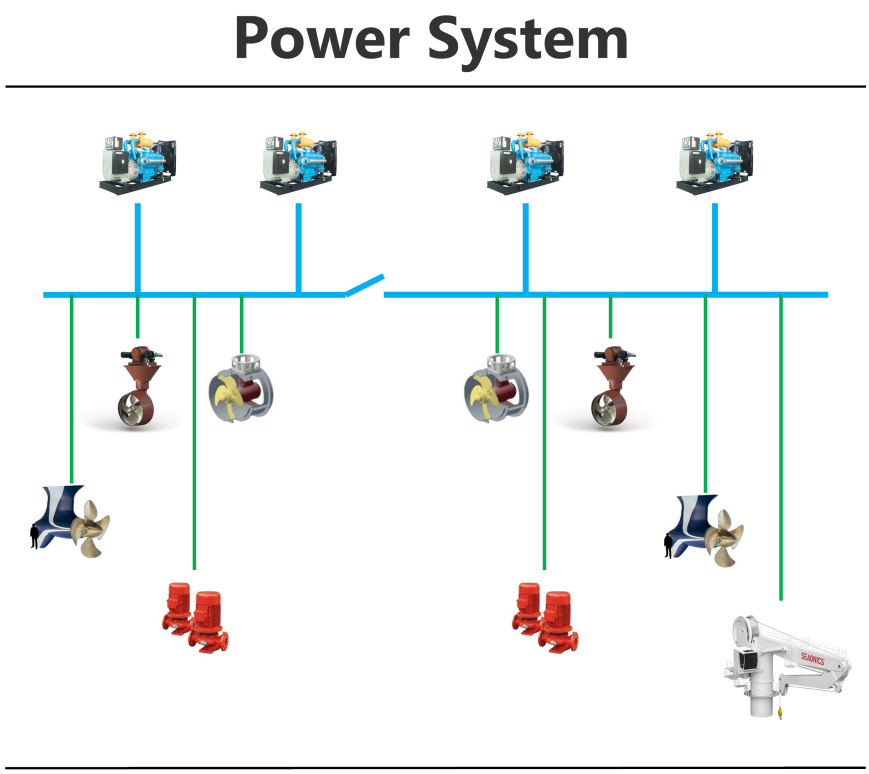

Figure 2.3: Example of the power system on a vessel

auxiliary systems, as well as to the DP control elements and position reference systems.

The thrusters on a DP vessel are often of the highest power consumers on board. The DP control system may demand large changes of power due to rapid changes in the weather conditions. The power generation must be flexible in order to provide power rapidly on demand while avoiding unnecessary fuel consumption. Many DP vessels are fitted with a diesel-electric power plant with all thrusters and consumers electrically powered from diesel engines driving alternators. A diesel engine and alternator is known as a diesel generator set. Tunnel-, azimuth- and azipull thrusters are usually driven by huge electric

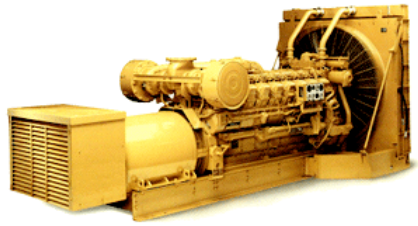

Figure 2.4: Figure of a typical diesel generator

motors, which gets their power from a diesel generator.

For main propulsion, a vessel may have twin screws that is driven directly by diesel engines, but diesel-electric powered main propulsion is getting more and more common. The DP control system also gets its power from the diesel generators. Should there be a failure in the normal power supply from the generators, the DP control system is protected from total black-out by an Uninterruptible Power Supply (UPS). This system provides a stable power supply that is not affected by short-term interruptions or fluctuations of the vessels power supply. It supplies the computers, control consoles, displays, alarms, and position reference systems. In the event of an interruption to the vessels main power supply, batteries will supply power to all of these systems for a minimum of 30 minutes [DNV, 2011].

2.2.1 Generators

The generators generating power on board a ship is in most cases a diesel driven engine that drives an alternator to generate AC. The generators are coupled to the main switchboard, and the number of generators on board have to be according to the redundancy requirements for the DP-class of the vessel. If the vessel is classified as a DP class 2 or 3, the number of generators must be at least two [Ådnanes, 2003]. This is because a single point of failure should not cause loss of heading or position. It seems common that there are 2 generators per main switchboard. This ensures that the vessel can operate with the two main switchboards separated, and still be protected from single point of failure in one of the generators.

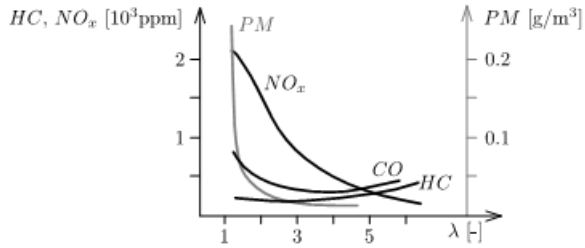

Figure 2.5: Engine-out emission of NO_x hydrocarbon (HC) and PM of a direct-injection Diesel engine as a function of air/fuel. This figure is taken directly from [Guzzella and Onder, 2010]

When in operation the vessel might not require that all generators are running. If large consumers are switched on which requires a new generator to start up, the PMS should automatically start the generator and phase it onto the main switch board [Radan, 2008] [Hansen, 2000]. It is worth noting that diesel generators on ships produce their AC with a frequency of 60Hz instead of 50Hz because of more fuel optimal working conditions. [Ådnanes, 2003].

Maritime diesel engines, because they have to produce AC with a given frequency, must operate at a steady RPM. The engines are controlled by a speed governor that changes the air/fuel ratio λ in the combustion chamber by increasing the fuel. Initially diesel engines had an approximately constant air supply while the fuel injected were varied by the actuator in order to change λ. More modern diesel engines that includes turbochargers complicates the dynamics. The turbocharger dynamics is relatively slow [Veksler et al., 2012b] [Guzzella and Onder, 2010].

The main pollutant species in the exhaust gas of a diesel engine are NO_x and particulate matter (PM or soot). The primary factor that affects the emissions is the air/fuel ratio λ, but injection timing, pressure and Exhaust Gas Recirculation (EGR) also play an important role. The importance of the latter three are emphasised in high fidelity models that considers the dynamics, and chemistry inside the combustion chamber as a function of crankshaft angle, shown in e.g [Aithal, 2010], [Widd, 2012], [Widd et al., 2008], [Widd et al., 2009]. Figure 2.5 is taken directly from [Guzzella and Onder, 2010] and it shows the engine-out emission of a direct-injection diesel engine as a function of air/fuel ratio. We see that both NO_x and PM emissions increase with the diesel engines load.

Generator Size (kW)	1/4 Load (gal/hr)	1/2 Load (gal/hr)	3/4 Load (gal/hr)	Full Load (gal/hr)
20	0.6	0.9	1.3	1.6
30	1.3	1.8	2.4	2.9
40	1.6	2.3	3.2	4.0
60	1.8	2.9	3.8	4.8
75	2.4	3.4	4.6	6.1
100	2.6	4.1	5.8	7.4
125	3.1	5.0	7.1	9.1
135	3.3	5.4	7.6	9.8
150	3.6	5.9	8.4	10.9
175	4.1	6.8	9.7	12.7
200	4.7	7.7	11.0	14.4
230	5.3	8.8	12.5	16.6
250	5.7	9.5	13.6	18.0
300	6.8	11.3	16.1	21.5
350	7.9	13.1	18.7	25.1
400	8.9	14.9	21.3	28.6
500	11.0	18.5	26.4	35.7
600	13.2	22.0	31.5	42.8
750	16.3	27.4	39.3	53.4
1000	21.6	36.4	52.1	71.1
1250	26.9	45.3	65.0	88.8
1500	32.2	54.3	77.8	106.5
1750	37.5	63.2	90.7	124.2
2000	42.8	72.2	103.5	141.9
2250	48.1	81.1	116.4	159.6

Figure 2.6: This table is taken from [DieselServiceAndSupply, 2013] and it shows an approximate fuel consumption for a generator of a given size

Static fuel consumption model

Figure 2.6 is taken from [DieselServiceAndSupply, 2013] and it shows the approximate fuel consumption for a diesel generator of a certain size. It would be advantageous to have an analytic function describing the fuel consumption of a given generator. In figure 2.7 the fuel consumption of a 1750kW generator is approximated by a polynomial of degree 2.

The 2_{nd} degree polynomial approximation of the fuel consumption of any given diesel generator as a function of it's load in kW is shown in equation (2.3). Where a_0, a_1 and a_2 are the constants that decides how the function will look and can be found by using e.g the *polyfit* function in `MATLAB`.

$$q_{G_k} = a_2 p_{G_k}^2 + a_1 p_{G_k} + a_0 \tag{2.3}$$

q_{G_k} is the fuel consumed by generator number k, p_{G_k} is the load generated by generator number k while a are constants that are used when fitting the polynomial to the data. This function will be used in this thesis as a model for how much fuel a generator consumes as a function of its produced power. It was

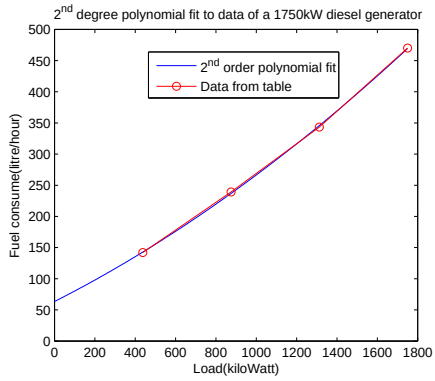

Figure 2.7: Fuel consumption of a 1750kW generator approximated with a polynomial of degree 2. Blue(polynomial of degree 2), Red(data from figure 2.6)

chosen to use a polynomial of degree 2, because of the slight curvature as seen in figure 2.7. It is important to capture this curvature in the model, because it states that the generator is more fuel efficient at higher loads. No dynamic models for the generators will be used in this thesis.

2.2.2 Bus-tie breaker

A bus-tie breaker is a device that is used to separate two main switchboards from each other.

Operating with the bus-tie breaker closed will distribute the load too all the active generators, and even out the load between the buses. One big drawback with closed bus-tie breaker is that a failure in one main switchboard can propagate to the other, ending in a black-ship situation that could have been avoided by running with open bus-tie breaker. It is because of this reason that some of vessels today operate with open bus-tie breaker while in critical DP-operations. As long as there exists equipment that can detect failures and isolate them so that they don't propagate through all the switchboards, the classification societies can accept to operate with closed bus-tie breaker in DP-class 2 operations. In DP-class 3 operations however, open bus-tie breaker is required [Ådnanes, 2003].

2.2.3 Main switchboard

A main switchboard or busbar, is where the power gets distributed to all the components on board the ship. The power comes in to the main switchboard from the diesel generators, and it is then distributed further to larger and smaller consumers.

The voltage in the switchboards can vary from 230V, 440V, 690V, 6.6kV and 11kV. There can also be more than one main switchboard on board a vessel. Typically a vessel is equipped with two main switchboards, one port and the other starboard. The two main switchboards are connected together with a bus-tie breaker which is either open or closed, depending on the operation and DP-class of the vessel as described in subsection 2.2.2. The number of switchboards a vessel is equipped with depends on the DP-class and redundancy requirements set by the classification societies. [DNV, 2011] [Ådnanes, 2003]

2.3 Control system

In Figure 2.8 we can see the general structure of the control system topology of a DP-system illustrated [Fossen, 2002]. The *Estimator* block is typically a Kalman-filter, which uses a mathematical model of the vessel to estimate non-measured states and disturbance, like current forces. Additionally, it's also common to feedforward the wind forces directly even though it is not shown here in Figure 2.8. The *Thruster Allocation* block shown in Figure 2.8 will be an optimization algorithm that takes the 3-dimensional thrust vector

$$\boldsymbol{\tau}_c = \begin{pmatrix} F_{surge} \\ F_{sway} \\ M_{yaw} \end{pmatrix}$$

from the DP-controller and turns it into thrust for each individual thruster

$$\mathbf{u} = \begin{pmatrix} \mathbf{u}_1 \\ \mathbf{u}_2 \\ \vdots \\ \mathbf{u}_n \end{pmatrix}$$

$$\mathbf{u}_i = \begin{pmatrix} u_{i,surge} \\ u_{i,sway} \end{pmatrix}$$

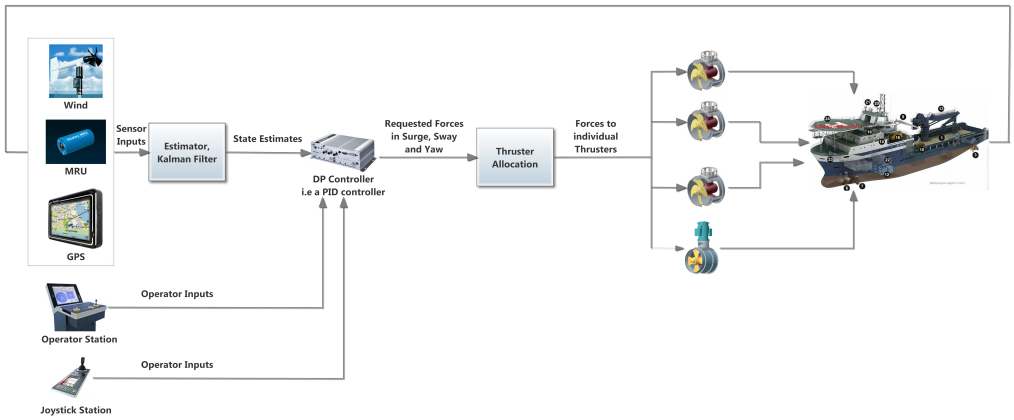

Figure 2.8: Structure of a DP control loop

Here $\mathbf{u}_i$ is a vector that contains the forces in surge and sway produced by thruster number i. An optimization algorithm is a good way to allocate thrust forces, because it creates a lot of freedom and opens up a lot of opportunities. You can for instance minimize the use of thrusters, change in thrust, turn rate, consider forbidden zones etc. The optimization algorithm should never allocate thrust forces in such a way that heading and/or position is lost.

CHAPTER 3

Thrust Allocation

3.1 Introduction

The generalized forces in surge, sway and yaw calculated by the high-level motion controller is denoted $\boldsymbol{\tau_c}$, while the generalized forces in surge, sway and yaw calculated by the thrust allocation algorithm is denoted $\boldsymbol{\tau}$. The two vectors $\boldsymbol{\tau_c}$ and $\boldsymbol{\tau}$ is on the form

$$\boldsymbol{\tau_c}, \boldsymbol{\tau} = \begin{pmatrix} F_{surge} \\ F_{sway} \\ M_{yaw} \end{pmatrix}$$

While $\boldsymbol{\tau_c}$ comes directly from the high-level motion controller, $\boldsymbol{\tau}$ is calculated through a function $l(\mathbf{u})$, where $\mathbf{u}$ is a vector of each individual thrusters forces in surge and sway direction and is on the form

$$\mathbf{u} = \begin{pmatrix} \mathbf{u}_1 \\ \mathbf{u}_2 \\ \vdots \\ \mathbf{u}_n \end{pmatrix}$$

where

$$\mathbf{u}_i = \begin{pmatrix} u_{i,surge} \\ u_{i,sway} \end{pmatrix}$$

here n is the total number of thrusters, i is thruster number i and $u_{i,surge}$ and $u_{i,sway}$ is thruster number i's forces in surge and sway direction respectively.

Since

$$(\boldsymbol{\tau_c} \wedge \boldsymbol{\tau}) \in \mathbb{R}^3$$

$$\mathbf{u}_i \in \mathbb{R}^2$$

and

$$\mathbf{u} \in \mathbb{R}^{2n}$$

$l(\mathbf{u})$ needs to be a function that maps $\mathbf{u}$ from $\mathbb{R}^{2n}$ to $\mathbb{R}^3$. $l(\mathbf{u})$ is derived from how the thrusters are arranged throughout the vessel, and maps each individual thrusters forces from "$\mathbf{u}$-space" to "$\boldsymbol{\tau}$-space". A common choice for $l(\mathbf{u})$ which will be used in this thesis as well is

$$l(\mathbf{u}) = \mathbf{B}\mathbf{u}$$

such that

$$\boldsymbol{\tau} = \mathbf{B}\mathbf{u}$$

where $\mathbf{B}$ is a $3 \times 2n$ matrix that describes how the thrusters exert forces and moments on the vessel. Figure 3.1 shows an illustration of $\mathbf{u}$-space, $\boldsymbol{\tau}$-space, and how $\mathbf{B}$ transforms $\mathbf{u}$ to $\boldsymbol{\tau}$.

Because of safety regulations, a vessel is usually over-actuated in terms of thrusters. This means that in principal you have infinitely many solutions as illustrated in figure 3.2. Since there are infinitely many solutions, formulating the thrust allocation problem as an optimization problem is a common way to go. This provides the possibility to find the thrust allocation solution which fulfils a user defined criterion, like

- low power
- high manoeuvrability
- low thruster fluctuations
- low fuel
- etc.

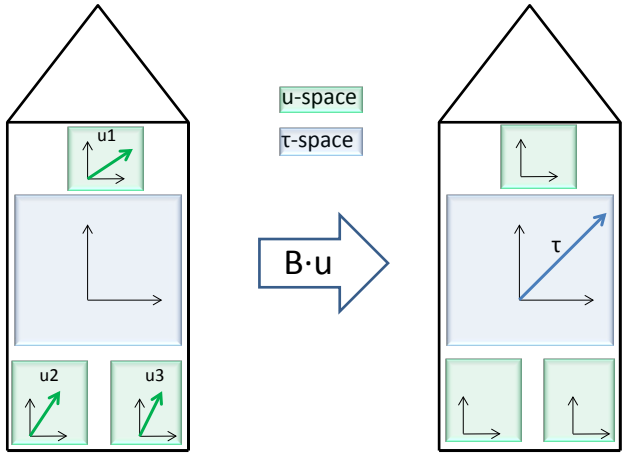

Figure 3.1: Illustration of $\mathbf{u}$-space, $\boldsymbol{\tau}$-space and how $\mathbf{B}$ transforms $\mathbf{u}$ to $\boldsymbol{\tau}$

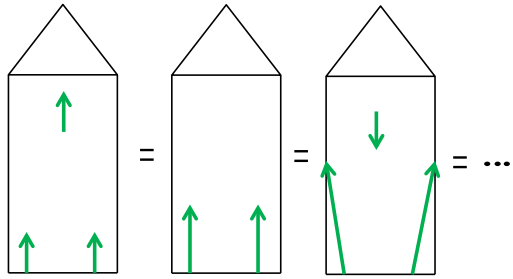

Figure 3.2: Illustration of how there exists many different solutions in **u**-space, which will give the same result in $\boldsymbol{\tau}$-space

with respect to certain constraints, e.g

- Maximum thrust capacity
- Maintaining DP capability
- Thrust- and azimuth rate changes
- Forbidden zones
- etc.

At its optimum, the optimization problem should ensure that $\boldsymbol{\tau} = \boldsymbol{\tau_c}$ if physically possible, since this should be the main objective of the thrust allocation algorithm. If $\boldsymbol{\tau}$ deviates significantly from $\boldsymbol{\tau_c}$, position and heading of the vessel can deviate from set-point, which may have severe consequences. It is advantageous if one can manage to formulate the optimization problem as a QP-problem, since these are well known and relatively easy to solve. If the QP-problem only has linear equality constraints the solution can be found directly, and if linear inequality constraints are introduced, an active-set algorithm [Nocedal and Wright, 2006] can be used to find the optimal solution.

3.2 Minimizing slack variables

As stated earlier the main objective of the thrust allocation should be to achieve $\boldsymbol{\tau_c} = \boldsymbol{\tau}$, and since we have chosen $\boldsymbol{\tau} = l(\mathbf{u}) = \mathbf{Bu}$ we get

$$\boldsymbol{\tau_c} = \mathbf{Bu} \tag{3.1}$$

So now $\mathbf{u}$ has to be chosen such that equation (3.1) is fulfilled. Since equation (3.1) has infinitely many solutions, it is reasonable to choose $\mathbf{u}$'s which minimizes $\|\boldsymbol{\tau_c} - \mathbf{Bu}\|_2^2$. This will give a least squares solution of (3.1) with respect to $\mathbf{u}$. However, because of physical limitations on the thrusters, equation (3.1) might not have any solution at all. Because of this, problem (3.2) is introduced.

$$\min_{\mathbf{u}\epsilon\mathbb{R}^{2n},\mathbf{s}\epsilon\mathbb{R}^3} \mathbf{s}^T\mathbf{Qs} \tag{3.2a}$$

$$\text{s.t}$$

$$\boldsymbol{\tau_c} - \mathbf{Bu} - \mathbf{s} = \mathbf{0} \tag{3.2b}$$

$$\mathbf{u}_{min} \leq \mathbf{u} \leq \mathbf{u}_{max} \tag{3.2c}$$

$$\boldsymbol{\Delta}\mathbf{u}_{min} \leq \boldsymbol{\Delta}\mathbf{u} \leq \boldsymbol{\Delta}\mathbf{u}_{max} \tag{3.2d}$$

$$\boldsymbol{\alpha}_{min} \leq \boldsymbol{\alpha} \leq \boldsymbol{\alpha}_{max} \tag{3.2e}$$

$$\boldsymbol{\Delta\alpha}_{min} \leq \boldsymbol{\Delta\alpha} \leq \boldsymbol{\Delta\alpha}_{max} \tag{3.2f}$$

The decision variables of problem (3.2) are $\mathbf{s}$ and $\mathbf{u}$, while $\mathbf{Q}$ is a square, symmetric and positive definite weighting matrix. Problem (3.2) tries to find the minimum values for $\mathbf{s}$, and values for $\mathbf{u}$ such that (3.2b)-(3.2f) are satisfied. The reason for introducing the slack variables comes from the physical constraints on the thrusters, given by (3.2c)-(3.2f). In situations where it is just not possible to use $\mathbf{u}$ in such a way that $\boldsymbol{\tau_c} = \boldsymbol{\tau}$, the slack variables are needed to ensure that the optimization problem has a feasible solution, by relaxing constraint (3.2b).

While constraint (3.2b) is linear, constraints (3.2c)-(3.2f) originally are not, because they describe physical absolute max/min and rate constraints on the thruster which is inherently non-linear. When $\mathbf{u}$ is chosen to be such that the $(2i-1)$ and $2i_{th}$ row is

$$\begin{pmatrix} u_{i,surge} \\ u_{i,sway} \end{pmatrix}$$

the thrust produced by thruster number i becomes

$$T_i = \sqrt{u_{i,surge}^2 + u_{i,sway}^2}$$

and the azimuth angle is

$$atan2(u_{i,sway}, u_{i,surge})$$

These equations are clearly non-linear in the decision variables $u_{i,surge}$ and $u_{i,sway}$. They can however be linearised, which is shown in subsection 3.3.2. This will make it possible to solve problems with these types of constraints relatively easy as a standard QP-problem with e.g an active-set algorithm.

Advantages of this formulation is that it is relatively easy to solve. It will produce solutions that keeps the thrusters within their physical limits, while also making sure that $\boldsymbol{\tau}$ is as close to $\boldsymbol{\tau_c}$ as possible. Problem (3.2) solves the initial problem of equation (3.1) not always having a solution because of physical limitations on the thrusters. But a big drawback is that this formulation has no say in how much thrust each thruster should provide, just that they should stay within certain limits. This is something that has to be accounted for, and one way to deal with this problem will be presented in section 3.3. This is also something that is recognized throughout the literature.

3.3 Minimizing thrust

In the previous section, slack variables were introduced into an optimization problem in order so make sure that the thrust allocation problem always produced feasible solutions, with the thrusters within their physical limitations. The problem was that it had no control over how much thrust each thruster actually produced. The most common way to solve this in the literature has been to introduce a quadratic penalty term on the thrusters, in this case $\mathbf{u}$. The term that is used is

$$\mathbf{u}^T\mathbf{G}\mathbf{u}$$

where $\mathbf{u}$ is still the thruster forces as explained earlier, and $\mathbf{G}$ is a square, symmetric and positive definite weighting matrix. This term can be seen throughout the literature e.g [Fossen and Johansen, 2006], [Johansen and Fossen, 2013], [Johansen et al., 2005], [Larsen, 2012], [Johansen et al., 2003], [Sørdalen, 1997, Wit, 2009], [Garus, 2004], [Jenssen and Realfsen, 2006], [Realfsen, 2009].

Unconstrained allocation will be presented first. Here inequality constraints will be excluded, to show how one can use the direct solution of a QP-problem to solve the thrust allocation problem in one iteration. The constrained allocation problem will then be presented, together with linearization of the inequality constraints describing the physical limitations on the thrusters.

3.3.1 Unconstrained allocation

In this section we will look at the unconstrained allocation case, where we take problem (3.2), add in the new term

$$\mathbf{u}^T\mathbf{G}\mathbf{u}$$

and exclude the inequality constraints from the optimization problem. This is to illustrate the direct solution of a QP-problem with only equality constraints.

In problem (3.3) we have an unconstrained allocation problem with the added penalty for using thrusters.

$$\min_{\mathbf{u}\epsilon\mathbb{R}^{2n},\mathbf{s}\epsilon\mathbb{R}^3} \mathbf{s}^T\mathbf{Q}\mathbf{s} + \mathbf{u}^T\mathbf{G}\mathbf{u} \tag{3.3a}$$

$$\text{s.t}$$

$$\boldsymbol{\tau_c} - \mathbf{B}\mathbf{u} - \mathbf{s} = \mathbf{0} \tag{3.3b}$$

This problem uses the term $\mathbf{s}^T\mathbf{Q}\mathbf{s}$ together with constraint (3.3b) to make sure that $\boldsymbol{\tau}$ is as close to $\boldsymbol{\tau_c}$ as possible, while the $\mathbf{u}^T\mathbf{G}\mathbf{u}$ term makes sure that the thrusters does not produce more thrust than necessary to make $\boldsymbol{\tau} \approx \boldsymbol{\tau_c}$. Generally one should make the weights in $\mathbf{Q} \gg \mathbf{G}$ to make sure that the top priority is to obtain the DP-order $\boldsymbol{\tau_c}$.

Before presenting the direct solution of problem (3.3) let us first rewrite it slightly.

$$\min_{\mathbf{x}\epsilon\mathbb{R}^{2n+3}} \mathbf{x}^T\mathbf{W}\mathbf{x} \tag{3.4a}$$

$$\text{s.t}$$

$$\mathbf{A}_{eq}\mathbf{x} - \mathbf{b}_{eq} = \mathbf{0} \tag{3.4b}$$

where

$$\mathbf{x} = \begin{pmatrix}\mathbf{u}\\ \mathbf{s}\end{pmatrix}$$

$$\mathbf{A}_{eq} = \begin{pmatrix}\mathbf{B} & \mathbf{I}\end{pmatrix}$$

$$\mathbf{b}_{eq} = \boldsymbol{\tau_c}$$

and

$$\mathbf{W} = \begin{pmatrix}\mathbf{G} & \mathbf{0}\\ \mathbf{0} & \mathbf{Q}\end{pmatrix}$$

This problem could be solved with an active-set algorithm but since it is a QP-problem with only linear equality constraints it always has the direct solution given by equation (3.5)

$$\underbrace{\begin{pmatrix} \mathbf{W} & \mathbf{A}_{eq}^T \\ \mathbf{A}_{eq} & \mathbf{0} \end{pmatrix}}_{\mathbf{K}} \begin{pmatrix} \mathbf{x} \\ \boldsymbol{\lambda} \end{pmatrix} = \begin{pmatrix} \mathbf{0} \\ \mathbf{b}_{eq} \end{pmatrix} \tag{3.5}$$

This equation is derived from the KKT-conditions which is described in detail in [Nocedal and Wright, 2006], with $\boldsymbol{\lambda}$ being the Lagrange multipliers.

Since $\mathbf{K}$ is a square matrix by construction, and if we can say that it is non-singular, the optimal solution to problem (3.4) will be given directly by equation (3.6)

$$\begin{pmatrix} \mathbf{x} \\ \boldsymbol{\lambda} \end{pmatrix} = \mathbf{K}^{-1} \begin{pmatrix} \mathbf{0} \\ \mathbf{b}_{eq} \end{pmatrix} \tag{3.6}$$

In [Nocedal and Wright, 2006] there is presented a proof for $\mathbf{K}$ being non-singular if $\mathbf{A}_{eq}$ has full row rank and the reduced Hessian is positive definite. Which means there is a unique solution for $\begin{pmatrix} \mathbf{x} \\ \boldsymbol{\lambda} \end{pmatrix}$ satisfying equation (3.6). Since $\mathbf{A}_{eq} = \begin{pmatrix} \mathbf{B} & \mathbf{I} \end{pmatrix}$, $\mathbf{A}_{eq}$ will have full row rank, if and only if $\mathbf{B}$ has full row rank. Usually though, for an over-actuated system, $\mathbf{B}$ will have full row rank. Rank-deficiency of the $\mathbf{B}$-matrix means that not all directions in $\boldsymbol{\tau_c}$ can be controlled through $\mathbf{Bu}$ [Johansen and Fossen, 2013]. The $\mathbf{B}$-matrix is constructed from the thruster arrangement of the vessel. Because of this, a rank-deficient $\mathbf{B}$-matrix can occur when a thruster failure is present. In case of $\mathbf{B}$ not having full rank, [Johansen and Fossen, 2013] presents a singular value decomposition approach, that allows for finding a solution even though $\mathbf{B}$ does not have full row rank.

Problem (3.4) in this section, shows how one can solve the thrust allocation problem in one time-step, by using the direct solution of a QP-problem. One obvious drawback is that the direct solution can only be used when the optimization problem has a quadratic objective function, and linear equality constraints. A quadratic objective function is almost always used, however, because of physical limitations on the thrusters one will need inequality constraints in the optimization problem, in order to accommodate these bounds. These constraints will be introduced in subsection 3.3.2.

3.3.2 Constrained allocation

In this subsection there will be presented two approaches for linearising the constraints imposed on the thrusters in problem (3.2). The first method is called *Polygon approximation* and comes from [Wit, 2009]. It is a way to obtain a set of linear equations that will constrain each thruster within their maximum thrust limits, but it will not take into account rate constraint and max/min angle constraints. The second approach from [Ruth, 2008], shown in **Linearized thrust magnitude- and directional constraints**, gives us a set of linear equations that has to be updated each time-step. The equations will take into account both absolute max/min thrust/angle and max/min thrust/angle rate constraints. If the given application does not need to take rate constraints into account the *Polygon approximation* can be used to constrain the thrusters. However, if rate constraints needs to be considered, which is usually the case, the second approach from [Ruth, 2008] can be used. The second approach is the one that will be used in this thesis, but both are presented.

Polygon approximation

Let us for simplicity look at the thrust produced by one single thruster. The thrust will be given by $T = \sqrt{u_{surge}^2 + u_{sway}^2}$, and if we put an upper bound on this thrust $T \leq T_{max}$ it will be a circular area if plotted in the space of u_{surge} and u_{sway}. The equation for this circular area given by u_{surge} and u_{sway} is shown in (3.7).

$$\sqrt{u_{surge}^2 + u_{sway}^2} \leq T_{max} \tag{3.7}$$

This equation is the non-linear constraint that we want to linearise. It is a circular area with radius T_{max}, and it contains the set of feasible thrust vectors that the thruster can produce.

One way to approximate a circle is by an N-sided polygon that fits inside the circle as illustrated in figure 3.3. Each side of the polygon represents a line that will be a linear constraint in our optimization problem. The number of sides of the polygon decides the number of constraints and the accuracy of the approximation. In figure 3.4 there is illustrated a circle with radius R, and a polygon with 8 sides approximating the circle. The line r goes from the centre of the circle and out to the line i, which represents one side of the polygon and

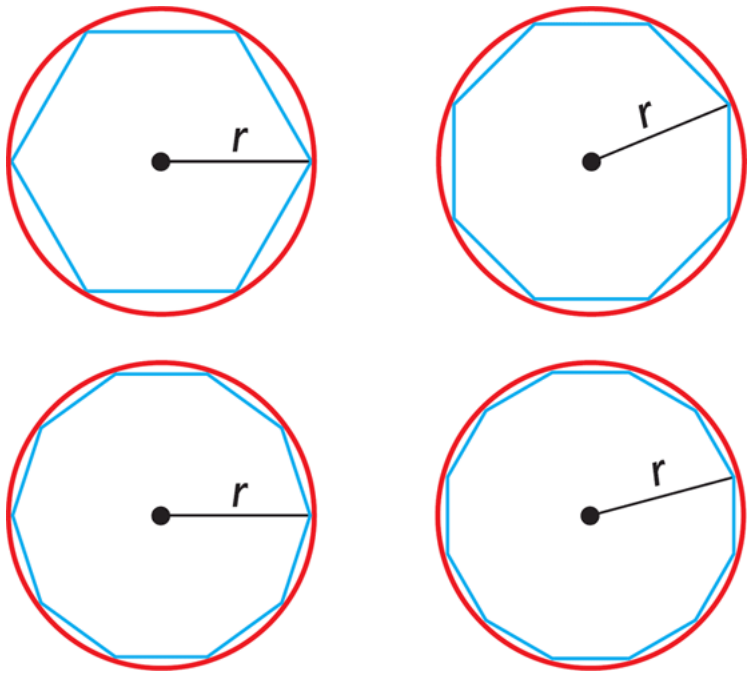

Figure 3.3: Illustration of polygons inside circles

line r is perpendicular to i. The length of line r is given by

$$r = R\cos(\theta/2) \tag{3.8}$$

where θ is the angle that spans one side of the N-sided polygon, and $\theta/2$ is the angle between the x_1-axis and the line r. The angle θ is given by $\theta = 2\pi/N$. Now, what is of interest is to find the equation for the line i.

The slope Δr of line r is given by

$$\Delta r = \frac{\sin(\theta/2)}{\cos(\theta/2)}$$

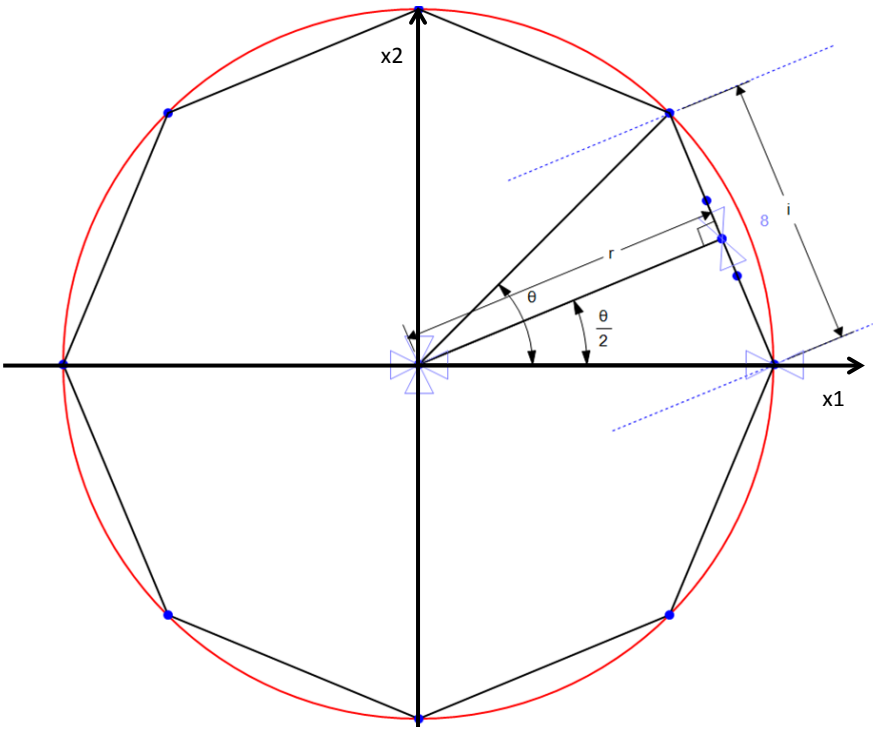

Figure 3.4: Circle approximated by a 8-sided polygon

since r is perpendicular to i the slope Δi of i is given by

$$\begin{aligned} \Delta i &= -\frac{1}{\Delta r} \\ &= -\frac{\cos(\theta/2)}{\sin(\theta/2)} \end{aligned} \tag{3.9}$$

The intersection-point p between line i and r is given by

$$\begin{aligned} x_1 &= r\cos(\theta/2) \\ x_2 &= r\sin(\theta/2) \end{aligned}$$

and we know that the equation for a straight line in the (x_1, x_2) plane is

$$x_2 = ax_1 + b$$

where a is the lines slope and b is the intersection-point. We already know the slope Δi of i such that

$$x_2 = \Delta i \cdot x_1 + b \tag{3.10}$$

Now by inserting our point p we can find b which is the only thing missing in our equation for line i.

$$x_2 = \Delta i \cdot x_1 + b$$

$$\underbrace{r\sin(\theta/2)}_{x_2} = \underbrace{-\frac{\cos(\theta/2)}{\sin(\theta/2)}}_{\Delta i} \cdot \underbrace{r\cos(\theta/2)}_{x_1} + b$$

$$b = r\sin(\theta/2) + \frac{\cos^2(\theta/2)}{\sin(\theta/2)} r \tag{3.11}$$

Now that we have the lines slope (3.9) and its intersection-point (3.11), we can simply insert it into (3.10) and get the equation for the first side of our N-sided polygon approximating our circle.

$$x_2 = -\frac{\cos(\theta/2)}{\sin(\theta/2)} \cdot x_1 + r\sin(\theta/2) + \frac{\cos^2(\theta/2)}{\sin(\theta/2)} r$$

$$x_2 + \frac{\cos(\theta/2)}{\sin(\theta/2)} \cdot x_1 = r\sin(\theta/2) + \frac{\cos^2(\theta/2)}{\sin(\theta/2)} r$$

$$x_2 \sin(\theta/2) + x_1 \cos(\theta/2) = r\sin^2(\theta/2) + r\cos^2(\theta/2)$$

$$x_2 \sin(\theta/2) + x_1 \cos(\theta/2) = r \tag{3.12}$$

Now, equation (3.12) only represents one side of the N-sided polygon. To generalize it such that we can find the equations of all the sides we can write

$$x_2 \sin(\theta_j) + x_1 \cos(\theta_j) = r \tag{3.13}$$

where

$$\theta_j = \frac{\pi}{N} + j\frac{2\pi}{N}, \quad \forall\ j = \{0, 1, 2, \ldots, N-1\}$$

and j represents side number j of the N-sided polygon. We observe that for any given N, θ_j is always known. r will be a constant for any j and (3.13) will then become a set of N linear equations. The same result, but without the derivation, have been used in [Wit, 2009].

Now that we have the equations for all the lines in our N-sided polygon approximating the circle given by (3.7), we can replace this constraint with the set of linear inequality constraint as shown in (3.14)

$$\mathbf{Cu} - \mathbf{r} \leq \mathbf{0} \tag{3.14}$$

where

$$\mathbf{C} = \begin{pmatrix} \mathbf{C}_1 & 0 & \dots & 0 \\ 0 & \mathbf{C}_2 & \dots & 0 \\ \vdots & \vdots & \ddots & \vdots \\ 0 & 0 & 0 & \mathbf{C}_n \end{pmatrix}, \mathbf{C}_j = \begin{pmatrix} \sin(\theta_0) & \cos(\theta_0) \\ \sin(\theta_1) & \cos(\theta_1) \\ \vdots & \vdots \\ \sin(\theta_{N-1}) & \cos(\theta_{N-1}) \end{pmatrix},$$

$$\mathbf{r} = \begin{pmatrix} \mathbf{r}_1 \\ \mathbf{r}_2 \\ \vdots \\ \mathbf{r}_n \end{pmatrix}, \mathbf{r}_j = \begin{pmatrix} r \\ r \\ \vdots \\ r \end{pmatrix},$$

$$\mathbf{u} = \begin{pmatrix} \mathbf{u}_1 \\ \mathbf{u}_2 \\ \vdots \\ \mathbf{u}_n \end{pmatrix}, \mathbf{u}_j = \begin{pmatrix} u_{j,surge} \\ u_{j,sway} \end{pmatrix}$$

Matrix $\mathbf{C}_j$ contains the N linear equations describing the N-sided polygon, in which the thrust produced by thruster number j is constrained. $\mathbf{r}_j$ is a vector that contains the maximum thrust value, specified by r for thruster number j. It is worth noting that the more sides the polygon has, the better the approximation of the circle (3.7) gets, but the number of equations will grow accordingly.

This approximation, or linearization gives a set of linear equations that will constrain the thrusters within their maximum thrust production limits. However, this approximation does not take into account rate-limitations on a thrusters, i.e a thruster cannot change it's thrust and/or direction infinitely fast from one time-step to the next. Linear inequality constraints that takes rate-limitations into account, are presented in the next sub-subsection.

Linearized thrust magnitude- and directional constraints

Since thrusters cannot change their direction and thrust arbitrarily fast from one time-step to the next, the thrust allocation algorithm has to take this into

account. This is usually done by the help of constraints in the optimization problem. The constraints will be inequality constraints, and they should be linear such that the optimization problem is still a QP-problem.

The linear inequality constraints presented in this sub-subsection are taken from [Ruth, 2008], and they are developed under the assumption that azimuth thrusters can only produce positive thrust. This assumption is also taken in this thesis.

The directional constraints of the thrusters are shown in equations (3.15), while the constraints on max/min thrust are shown in equations (3.16).

$$\sin(\alpha_{j,-})u_{j,surge} - \cos(\alpha_{j,-})u_{j,sway} \leq c_2|\cos(\alpha_{j,-})|(T_{j,+} - T_{j,-}) \tag{3.15a}$$
$$-\sin(\alpha_{j,+})u_{j,surge} + \cos(\alpha_{j,+})u_{j,sway} \leq c_2|\cos(\alpha_{j,+})|(T_{j,+} - T_{j,-}) \tag{3.15b}$$

$$-\cos(\alpha_{j,0})u_{j,surge} - \sin(\alpha_{j,0})u_{j,sway} \leq -T_{j,-} \tag{3.16a}$$
$$\cos(\alpha_{j,-})u_{j,surge} + \sin(\alpha_{j,-})u_{j,sway} \leq \cos(\alpha_{j,-} - \alpha_{j,0})T_{j,+} \tag{3.16b}$$
$$\cos(\alpha_{j,+})u_{j,surge} + \sin(\alpha_{j,+})u_{j,sway} \leq \cos(\alpha_{j,+} - \alpha_{j,0})T_{j,+} \tag{3.16c}$$

c_2 is a small constant, which together with the term $c_2|cos(\alpha_-)|(T_+ - T_-)$ allows for thrust in a small area around $\mathbf{u}_j = 0$, so that the thruster can rotate around zero thrust. [Ruth, 2008] suggests $c_2 = 0.001$ which is used in this thesis as well. T_+, T_-, α_+ and α_- are the values that decides how much the thrust and angle can change from one time-step to the next. They are chosen according to equations (3.17).

$$T_{j,+} = \min\left\{T_{j,0} + \Delta t \cdot \dot{T}_{j,max}, T_{j,max}\right\} \tag{3.17a}$$
$$T_{j,-} = \max\left\{T_{j,0} - \Delta t \cdot \dot{T}_{j,max}, T_{j,min}\right\} \tag{3.17b}$$
$$\alpha_{j,+} = \min\left\{\alpha_{j,0} + \Delta t \cdot \dot{\alpha}_{j,max}, \alpha_{j,max}\right\} \tag{3.17c}$$
$$\alpha_{j,-} = \max\left\{\alpha_{j,0} - \Delta t \cdot \dot{\alpha}_{j,max}, \alpha_{j,min}\right\} \tag{3.17d}$$

Here $T_{j,0}$ and $\alpha_{j,0}$ are the thrust and angle from the previous time-step, while $\dot{T}_{j,max}$ and $\dot{\alpha}_{j,max}$ are the physically maximum possible change in thrust and angle per second. $T_{j,max}$ and $T_{j,min}$ are the absolute maximum and minimum limits on how much thrust one thruster can produce, while $\alpha_{j,max}$ and $\alpha_{j,min}$ are the physical maximum and minimum possible angle for each thruster. Δt is the sample time at which the thrust allocation algorithm is run. Since the decision variables on the thrusters given by vector $\mathbf{u}$ is a thrusters forces in both

surge and sway direction, the angle of thruster number i , α_i is found after the optimization problem by

$$\alpha_i = atan2\left(u_{i,sway}, u_{i,surge}\right)$$

where $atan2$ is the four quadrant arctangent function.

The thruster constraints from equations (3.15) and (3.16) can be put on matrix-form as shown in (3.18), in order to formulate the optimization problem as a standard QP-problem with both equality and inequality constraints.

$$\begin{pmatrix} \mathbf{C} \\ \mathbf{D} \end{pmatrix} \mathbf{u} - \begin{pmatrix} \mathbf{c} \\ \mathbf{d} \end{pmatrix} \leq \mathbf{0} \tag{3.18}$$

where $\mathbf{C} = \begin{pmatrix} \mathbf{C}_1 & 0 & \dots & 0 \\ 0 & \mathbf{C}_2 & \dots & 0 \\ \vdots & \vdots & \ddots & \vdots \\ 0 & 0 & \dots & \mathbf{C}_n \end{pmatrix}$ and $\mathbf{C}_j = \begin{pmatrix} \sin(\alpha_{j,-}) & -\cos(\alpha_{j,-}) \\ -\sin(\alpha_{j,+}) & \cos(\alpha_{j,+}) \end{pmatrix}$, $\mathbf{c} = \begin{pmatrix} \mathbf{c}_1 \\ \mathbf{c}_2 \\ \vdots \\ \mathbf{c}_n \end{pmatrix}$ and $\mathbf{c}_j = \begin{pmatrix} c_2 |\cos(\alpha_{j,-})| (T_{j,+} - T_{j,-}) \\ c_2 |\cos(\alpha_{j,+})| (T_{j,+} - T_{j,-}) \end{pmatrix}$, $\mathbf{D} = \begin{pmatrix} \mathbf{D}_1 & 0 & \dots & 0 \\ 0 & \mathbf{D}_2 & \dots & 0 \\ \vdots & \vdots & \ddots & \vdots \\ 0 & 0 & \dots & \mathbf{D}_n \end{pmatrix}$ and $\mathbf{D}_j = \begin{pmatrix} -\cos(\alpha_{j,0}) & -\sin(\alpha_{j,0}) \\ \cos(\alpha_{j,-}) & \sin(\alpha_{j,-}) \\ \cos(\alpha_{j,+}) & \sin(\alpha_{j,+}) \end{pmatrix}$, $\mathbf{d} = \begin{pmatrix} \mathbf{d}_1 \\ \mathbf{d}_2 \\ \vdots \\ \mathbf{d}_n \end{pmatrix}$ and $\mathbf{d}_j = \begin{pmatrix} -T_{-,j} \\ \cos(\alpha_{j,-} - \alpha_{j,0}) T_{j,+} \\ \cos(\alpha_{j,+} - \alpha_{j,0}) T_{j,+} \end{pmatrix}$

$\mathbf{u}$ is still the vector containing all the thruster forces, and the $\mathbf{C}$-matrix in this sub-subsection should not be confused with the $\mathbf{C}$-matrix in the previous sub-subsection. It is important to note that these constraints needs to be updated before each optimization.

Figure 3.3.2 shows an illustration of how the constraints limit the possible thrust vectors from one time-step to the next.

The derivation of these constraints is not shown, but it is similar to the way the linear inequality constraints are derived in the polygon approximation from the previous sub-subsection.

Formulating the optimization problem

Now that the linear constraints on the physical limitations on the thrusters is in place, they can be added to the optimization problem as shown in problem (3.19)

$$\min_{\mathbf{x}\epsilon\mathbb{R}^{2n+3}} \mathbf{x}^T\mathbf{W}\mathbf{x} \tag{3.19a}$$

$$\text{s.t}$$

$$\mathbf{A}_{eq}\mathbf{x} - \mathbf{b}_{eq} = \mathbf{0} \tag{3.19b}$$

$$\mathbf{A}_{ineq}\mathbf{x} - \mathbf{b}_{ineq} \leq \mathbf{0} \tag{3.19c}$$

where

$$\mathbf{x} = \begin{pmatrix} \mathbf{u} \\ \mathbf{s} \end{pmatrix}$$

$$\mathbf{W} = \begin{pmatrix} \mathbf{G} & \mathbf{0} \\ \mathbf{0} & \mathbf{Q} \end{pmatrix}$$

$$\mathbf{A}_{eq} = \begin{pmatrix} \mathbf{B} & \mathbf{I} \end{pmatrix}$$

$$\mathbf{b}_{eq} = \boldsymbol{\tau_c}$$

while $\mathbf{A}_{ineq}$ and $\mathbf{b}_{ineq}$ can be chosen to fit equation (3.14) or (3.18). However, since rate constraints should be taken into account to in this thesis, $\mathbf{A}_{ineq}$ and $\mathbf{b}_{ineq}$ will be chosen to fit equation (3.18). Thus

$$\mathbf{A}_{ineq} = \begin{pmatrix} \mathbf{C} & \mathbf{0} \\ \mathbf{D} & \mathbf{0} \end{pmatrix}$$

and

$$\mathbf{b}_{ineq} = \begin{pmatrix} \mathbf{c} \\ \mathbf{d} \end{pmatrix}$$

This optimization problem, because of its objective function, will seek to minimize the amount of thrust produced by the thrusters. Because of the constraints the thrusters will stay within their limits, and it will make $\boldsymbol{\tau}$ as close to $\boldsymbol{\tau_c}$ as possible. The weights in $\mathbf{Q}$ are still larger than the weights in $\mathbf{G}$. However, there is still some freedom when choosing the weights in $\mathbf{G}$. You could weight the thrusters equally much, which will minimize the total amount of thrust produced. Or you could weight each thruster by the inverse of its maximum thrust

capability. This will make the thrusters produce equal thrust in percentage of their maximum thrust producing capacity.

The next step now will be to formulate an optimization problem which minimizes the amount of power in kW that the thrusters use. Because of the non-linear relationship between thrust and power, minimizing the thrust does not necessarily imply minimizing power.

3.4 Minimizing power

Minimizing power instead of thrust is recognized throughout the literature e.g [Ruth, 2008, Wit, 2009, Larsen, 2012, Veksler et al., 2012a, Veksler et al., 2012b, Jenssen and Realfsen, 2006]. When we wish to minimize power used by the thrusters, we need to introduce a term in the objective function that accurately enough describes the amount of power consumed by each thruster.

What we want is an optimization problem with an objective function on the following form

$$J = \mathbf{s}^T \mathbf{Q} \mathbf{s} + \sum_{i=1}^{n} p_{T_i}$$

where p_{T_i} is the power consumed by thruster number i. An optimization problem with this objective function will minimize the sum of power consumed by all the thrusters, and it would be advantageous if it was quadratic in the decision variables, such that it is still a QP-problem.

The relationship between thrust and power consumed by thruster number i is as follows

$$p_{T_i} = |T_i|^{3/2} \tag{3.20}$$

where

$$T_i = \sqrt{u_{i,surge}^2 + u_{i,sway}^2} \tag{3.21}$$

This means that the objective function is not a quadratic function in our decision variables. If we want to use p_{T_i} as it is, a non-linear solver must be used in order to solve the optimization problem. However, we notice that if we can make equation (3.20) quadratic in T it will also be quadratic in our decision variables since

$$T_i^2 = u_{i,surge}^2 + u_{i,sway}^2$$

In [Ruth, 2008], the quadratic approximation of (3.20) shown in (3.22), is used.

$$p_{T_i} \approx p_{T_i}^Q = \frac{T_i^2}{\sqrt{|T_{i,prev}|}} \tag{3.22}$$

This approximation will be used throughout this thesis, and the super-script ^{Q} is to indicate that it is quadratic approximation in the decision variables given by $\mathbf{u}$. For a more in-depth analyses on the derivation of the approximation please see [Ruth, 2008].

Now that we can express p_{T_i} as a quadratic function in the decision variables, we can set up the objective function of our power minimizing optimization problem as shown in equation (3.23).

$$J = \mathbf{s}^T\mathbf{Q}\mathbf{s} + \sum_{i=1}^{n} \frac{1}{\gamma_i} p_{T_i}^Q \tag{3.23}$$

here γ_i is a weighting factor. If one chooses $\gamma_i = 1$ the total amount of power consumed by all the thrusters will be minimized. If one chooses $\gamma_i = p_{T_i,max}$ where $p_{T_i,max}$ is the maximum possible power consumed by thruster number i, the thrusters will consume percentage wise equal amounts of power.

Objective function J given by equation (3.23), can be put on matrix form in the following way

$$\begin{aligned}
J &= \mathbf{s}^T\mathbf{Q}\mathbf{s} + \sum_{i=1}^{n} \frac{1}{\gamma_i} p_{T_i}^Q \\
&= \mathbf{s}^T\mathbf{Q}\mathbf{s} + \sum_{i=1}^{n} \frac{1}{\gamma_i} \frac{T_i^2}{\sqrt{|T_{i,prev}|}} \\
&= \mathbf{s}^T\mathbf{Q}\mathbf{s} + \sum_{i=1}^{n} \frac{1}{\gamma_i} \frac{u_{i,surge}^2 + u_{i,sway}^2}{\sqrt{|T_{i,prev}|}} \\
&= \mathbf{s}^T\mathbf{Q}\mathbf{s} + \sum_{i=1}^{n} \frac{1}{\gamma_i} \frac{\mathbf{u}_i^T\mathbf{u}_i}{\sqrt{|T_{i,prev}|}} \\
&= \mathbf{s}^T\mathbf{Q}\mathbf{s} + \mathbf{u}^T\mathbf{H}\mathbf{u}
\end{aligned} \tag{3.24}$$

where

$$\mathbf{u} = \begin{pmatrix} \mathbf{u}_1 \\ \mathbf{u}_2 \\ \vdots \\ \mathbf{u}_n \end{pmatrix}$$

$$\mathbf{u}_i = \begin{pmatrix} u_{i,surge} \\ u_{i,sway} \end{pmatrix}$$

and

$$\mathbf{H} = \begin{pmatrix} \frac{1}{\gamma_1\sqrt{T_{1,prev}}} & 0 & 0 & \dots & 0 \\ 0 & \frac{1}{\gamma_1\sqrt{T_{1,prev}}} & 0 & \vdots & \vdots \\ \vdots & \vdots & \ddots & \vdots & \vdots \\ 0 & \dots & \dots & \frac{1}{\gamma_n\sqrt{T_{n,prev}}} & 0 \\ 0 & \dots & \dots & 0 & \frac{1}{\gamma_n\sqrt{T_{n,prev}}} \end{pmatrix}$$

Notice that since $T_{i,prev}$ is included in the **H**-matrix, it has to be updated each time the thrust allocation algorithm is run.

3.4.1 Power constraints

In order to make sure that the thrusters does not consume more power than available on the bus, constraints on p_{T_i} should be included in the thrust allocation problem. These types of constraints are also presented in [Ruth, 2008, Jenssen and Realfsen, 2006].

The amount of load on bus number j can be defined as

$$p_{bus_j} = \sum_{i=1}^{n} (\mathbf{M}_{ji} p_{T_i}) + p_{ext_j} \tag{3.25}$$

where p_{ext_j} is the load on bus j because of external consumers, other than the thrusters and

$$\mathbf{M} = \begin{pmatrix} m_{11} & m_{12} & \dots & m_{1n} \\ m_{21} & m_{22} & \dots & m_{2n} \\ \vdots & \vdots & \vdots & \vdots \\ m_{j1} & m_{j2} & \dots & m_{jn} \end{pmatrix}$$

the **M**-matrix has values 1 and 0, and it describes which thruster is connected to which bus. j is the number of bus bars, and n is the number of thrusters.

The amount of load on bus j can never be higher than the maximum available power, given by $p_{bus_j}^{avail}$. This gives the constraint

$$\begin{aligned} p_{bus_j} &\leq p_{bus_j}^{avail} \\ \sum_{i=1}^{n}(\mathbf{M}_{ji}p_{T_i}) + p_{ext_j} &\leq p_{bus_j}^{avail} \\ \sum_{i=1}^{n}(\mathbf{M}_{ji}p_{T_i}) &\leq p_{bus_j}^{avail} - p_{ext_j} \end{aligned} \tag{3.26}$$

notice that equation (3.26) is non-linear in the decision variables. If we wish to formulate a QP-problem, this equation needs to be linearised with respect to the decision variables in $\mathbf{u}$.

Since

$$p_{T_i} = |T_i|^{3/2}$$

and

$$T_i = \sqrt{u_{i,surge}^2 + u_{i,sway}^2}$$

T_i is always positive so we can set

$$\begin{aligned} p_{T_i} &= T_i^{3/2} \\ &= (u_{i,surge}^2 + u_{i,sway}^2)^{3/4} \\ &= (\mathbf{u}_i^T\mathbf{u}_i)^{3/4} \end{aligned} \tag{3.27}$$

where $\mathbf{u}_i = \begin{pmatrix} u_{i,surge} \\ u_{i,sway} \end{pmatrix}$ and i is thruster number i.

Inserting (3.27) into (3.26) gives

$$\sum_{i=1}^{n}\left(\mathbf{M}_{ji}(\mathbf{u}_i^T\mathbf{u}_i)^{3/4}\right) \leq p_{bus_j}^{avail} - p_{ext_j}$$

Let us set

$$f(\mathbf{u}_i) = \mathbf{M}_{ji}(\mathbf{u}_i^T\mathbf{u}_i)^{3/4}$$

and find a first order taylor approximation $f^L(\mathbf{u}_i)$ of $f(\mathbf{u}_i)$ around the thruster values from the previous time-step, $\mathbf{u}_{i,prev}$.

$$\begin{aligned}
f(\mathbf{u}_i) &\approx f(\mathbf{u}_{i,prev}) + \nabla f^T|_{\mathbf{u}_{i,prev}} \cdot (\mathbf{u}_i - \mathbf{u}_{i,prev}) \\
&= \underbrace{\mathbf{M}_{ji}(\mathbf{u}_{i,prev}^T \mathbf{u}_{i,prev})^{3/4}}_{f(\mathbf{u}_{i,prev})} + \underbrace{\mathbf{M}_{ji}\frac{3 \cdot \mathbf{u}_{i,prev}^T}{2(\mathbf{u}_{i,prev}^T \mathbf{u}_{i,prev})^{1/4}}}_{\nabla f^T|_{\mathbf{u}_{i,prev}}} \cdot (\mathbf{u}_i - \mathbf{u}_{i,prev}) \\
&= \mathbf{M}_{ji}(\mathbf{u}_{i,prev}^T \mathbf{u}_{i,prev})^{3/4} + \mathbf{M}_{ji}\frac{3 \cdot \mathbf{u}_{i,prev}^T}{2(\mathbf{u}_{i,prev}^T \mathbf{u}_{i,prev})^{1/4}}\mathbf{u}_i \\
&- \mathbf{M}_{ji}\frac{3}{2(\mathbf{u}_{i,prev}^T \mathbf{u}_{i,prev})^{1/4}}\mathbf{u}_{i,prev}^T \mathbf{u}_{i,prev} \\
&= \mathbf{M}_{ji}(\mathbf{u}_{i,prev}^T \mathbf{u}_{i,prev})^{3/4} + \mathbf{M}_{ji}\frac{3 \cdot \mathbf{u}_{i,prev}^T}{2(\mathbf{u}_{i,prev}^T \mathbf{u}_{i,prev})^{1/4}}\mathbf{u}_i \\
&- \mathbf{M}_{ji}\frac{3}{2}(\mathbf{u}_{i,prev}^T \mathbf{u}_{i,prev})^{3/4} \\
&= \mathbf{M}_{ji}\frac{3 \cdot \mathbf{u}_{i,prev}^T}{2(\mathbf{u}_{i,prev}^T \mathbf{u}_{i,prev})^{1/4}}\mathbf{u}_i - \mathbf{M}_{ji}\frac{(\mathbf{u}_{i,prev}^T \mathbf{u}_{i,prev})^{3/4}}{2} \\
&= f^L(\mathbf{u}_i)
\end{aligned}$$

$f^L(\mathbf{u}_i)$ is the linearization of $f(\mathbf{u}_i)$, and we can now insert it into equation (3.26) as shown in (3.28)

$$\sum_{i=1}^{n} f^L(\mathbf{u}_i) \leq p_{bus_j}^{avail} - p_{ext_j}$$

$$\sum_{i=1}^{n}\left(\mathbf{M}_{ji}\frac{3 \cdot \mathbf{u}_{i,prev}^T}{2(\mathbf{u}_{i,prev}^T \mathbf{u}_{i,prev})^{1/4}}\mathbf{u}_i - \mathbf{M}_{ji}\frac{(\mathbf{u}_{i,prev}^T \mathbf{u}_{i,prev})^{3/4}}{2}\right) \leq p_{bus_j}^{avail} - p_{ext_j} \tag{3.28}$$

Equation (3.28) is now a linear equation in the decision variables, and can be used as an inequality constraint in a QP-problem. In order to use equation (3.28) as a constraint in the optimization problem, it is worth noting that one has to update the constraint for each time-step. The constraint is linearised about the thruster values from the previous time-step, each iteration. This linearization is also done in [Ruth, 2008], and he also argues for the accuracy of the linearization to be good enough, since there are rate constraints on the thrusters.

The maximum available power on bus number j, given by $p_{bus_j}^{avail}$ is decided by the size and number of generators connected to the bus.

3.4.2 Formulating the optimization problem

Given the objective function (3.23) and power constraint (3.28), an optimization problem can be formulated as shown in (3.29).

$$\min_{\mathbf{x}\epsilon\mathbb{R}^{2n+3}} \mathbf{x}^T\mathbf{W}\mathbf{x} \tag{3.29a}$$

s.t

$$\mathbf{A}_{eq}\mathbf{x} - \mathbf{b}_{eq} = \mathbf{0} \tag{3.29b}$$

$$\mathbf{A}_{ineq}\mathbf{x} - \mathbf{b}_{ineq} \leq \mathbf{0} \tag{3.29c}$$

$$\sum_{i=1}^{n} f^L(\mathbf{u}_i) \leq p_{bus_j}^{avail} - p_{ext_j} \tag{3.29d}$$

where

$$\mathbf{x} = \begin{pmatrix} \mathbf{u} \\ \mathbf{s} \end{pmatrix}$$

$$\mathbf{W} = \begin{pmatrix} \mathbf{H} & \mathbf{0} \\ \mathbf{0} & \mathbf{Q} \end{pmatrix}$$

and the $\mathbf{H}$-matrix is the one used in equation (3.24). Constraint (3.29b) and (3.29c) are the same as in problem (3.19). Constraint (3.29d) is the constraint which specifies how much power each thruster can consume, and it comes from equation (3.28).

Problem (3.29) has both a quadratic objective function, and linear constraints which makes it a QP-problem. It minimizes the power consumed by each thruster, makes sure that the rate constraints are not violated, tries to make $\boldsymbol{\tau}$ as close to $\boldsymbol{\tau_c}$ as possible and makes sure that the thrusters does not consume more power than available on the bus.

3.5 Minimizing fuel consumption

In section 3.2 slack variables were introduced into an optimization problem in order to ensure a feasible solution of the thrust allocation problem, even though $\boldsymbol{\tau} = \boldsymbol{\tau_c}$ was not possible. Furthermore, section 3.3 introduced a new term into

the objective function, describing the total amount of thrust produced by the thrusters, and included constraints specifying the physical limitations on the thrusters. This optimization problem solves the thrust allocation problem while using as little thrust as possible and making sure that the thrusters stay within their physical limitations. Section 3.4, instead of minimizing thrust, minimizes the total amount of power consumed by the thrusters. The optimization problem also included constraints which makes sure that the thrusters does not consume more power than available on the bus.

The objective of this section, is to derive an expression for the fuel consumed by the generators as a function of the thrusters, and the external power on the bus which the generators are connected to. There will also be formulated an optimization problem that instead of minimizing thrust, or power consumed by the thrusters, minimizes the fuel consumed by the generators. This means that we want and objective function on the following form

$$J = \mathbf{s}^T \mathbf{Q} \mathbf{s} + g(\boldsymbol{q_G})$$

where $\boldsymbol{q_G} \in \mathbb{R}^l$ is a vector containing the fuel consumption of every generator and l is the number of generators. We would like $g(\boldsymbol{q_G})$ to be a quadratic function in the decision variables $\mathbf{u}$, so that a fuel minimizing QP-problem can be formulated. This will be done in this section and subsection 3.5.1.

By equation (2.3), we have an expression for how much fuel a generator consumes as a function of its produced power. The amount of load on bus number j is given by

$$p_{bus_j} = \sum_{i=1}^{n} \mathbf{M}_{ji} p_{T_i}^Q + p_{ext_j}$$

if we use the quadratic approximation from [Ruth, 2008] of p_{T_i}. The load that a generator needs to generate in order to supply the demand on the bus, depends on the number of generators connected to the bus and how they should share the load. In this thesis it is assumed that the load sharing between generators connected to the same bus is symmetric, meaning they generate the same amount of power. Another assumption is that the vessel always operates with open bus-tie breaker. Load sharing and PMS in general is discussed more in detail in [Radan, 2008] and [Hansen, 2000].

The equation describing the load sharing of the generators in this thesis is as follows

$$\mathbf{E}\boldsymbol{p_G} = \begin{pmatrix} \boldsymbol{p_{bus}} \\ \mathbf{0} \end{pmatrix} \tag{3.30}$$

where $\boldsymbol{p_G}$ is a vector of the load generated by each generator, $\boldsymbol{p_{bus}}$ is the load on the bus bars and $\mathbf{E}$ is a matrix that describes which generator is connected to which bus bar, and it also makes sure that the load sharing between the generators is symmetric. The zero in the vector on the right hand side of equation (3.30) is there to form equations which states that generators connected to the same bus, should have the same load. $\boldsymbol{p_{bus}}$ form equations that says the sum of all generators connected to the same bus, should equal the load on that bus. In order to find how much power each generator has to generate, we simply use the inverse of $\mathbf{E}$ in the following way

$$\boldsymbol{p_G} = \mathbf{E}^{-1} \begin{pmatrix} \boldsymbol{p_{bus}} \\ \mathbf{0} \end{pmatrix} \tag{3.31}$$

As long as there is at least one generator connected to each busbar, $\mathbf{E}$ will have full rank, and equation (3.31) will have a unique solution. However, if one busbar does not have any generators connected to it, $\mathbf{E}$ will lose rank and its pseudo-inverse can be used instead. Since the load sharing is assumed symmetric, the pseudo-inverse will give correct solutions because of the least-squares problem the pseudo-inverse solves.

The load generated by generator number k becomes

$$\begin{aligned} p_{G_k} &= \sum_{j=1}^{m} (\mathbf{E}^{-1})_{kj} p_{bus_j} \\ p_{G_k} &= \sum_{j=1}^{m} \sum_{i=1}^{n} (\mathbf{E}^{-1})_{kj} \mathbf{M}_{ji} p_{T_i}^{Q} + p_{ext_j} \end{aligned} \tag{3.32}$$

where m is the number of busbars, j is bus number j and i is thruster number i. We immediately notice that when we use a quadratic approximation of $p_{T_i}^{Q}$, the load on generator k, p_{G_k}, also becomes quadratic in the decision variables. This means that if we linearise equation (2.3) with respect to p_{G_k}, it will be quadratic in the decision variables as well. Because of this the function $g(\boldsymbol{q_G})$ in the objective function, has to be linear in q_{G_k} so that it becomes quadratic in the decision variables.

From equation (2.3) we have that

$$q_{G_k} = a_2 p_{G_k}^2 + a_1 p_{G_k} + a_0$$

linearising this with respect to p_{G_k} around $p_{G_{k,prev}}$ each time-step gives

$$\begin{aligned}
q_{G_k} &\approx (a_2 p_{G_{k,prev}}^2 + a_1 p_{G_{k,prev}} + a_0) + (2a_2 p_{G_{k,prev}} + a_1) \cdot (p_{G_k} - p_{G_{k,prev}}) \\
&= (2a_2 p_{G_{k,prev}} + a_1) p_{G_k} - a_2 p_{G_{k,prev}}^2 + a_0 \\
&= (2a_2 p_{G_{k,prev}} + a_1) \left(\sum_{j=1}^{m} \sum_{i=1}^{n} (\mathbf{E}^{-1})_{kj} \mathbf{M}_{ji} p_{T_i}^Q + p_{ext_j} \right) - a_2 p_{G_{k,prev}}^2 + a_0 \\
&= (2a_2 p_{G_{k,prev}} + a_1) \left(\sum_{j=1}^{m} \sum_{i=1}^{n} (\mathbf{E}^{-1})_{kj} \mathbf{M}_{ji} \frac{(u_{i,surge}^2 + u_{i,sway}^2)}{\sqrt{|T_{i,prev}|}} + p_{ext_j} \right) \\
&\quad - a_2 p_{G_{k,prev}}^2 + a_0 \qquad (3.33) \\
&= q_{G_k}^Q
\end{aligned}$$

$q_{G_k}^Q$ is the fuel consumed by generator number k, and it is quadratic in the decision variables. We see that equation (3.33) is quadratic in the decision variables, and it describes how much fuel generator k consumes. If we set

$$g(\boldsymbol{q_G}) = \sum_{k=1}^{l} \frac{1}{\mu_k} q_{G_k}^Q$$

where μ_k is a scaling factor, we can set up the objective function given by equation (3.34)

$$J = \mathbf{s}^T \mathbf{W} \mathbf{s} + \sum_{k=1}^{l} \frac{1}{\mu_k} q_{G_k}^Q \qquad (3.34)$$

which is a quadratic function in the decision variables $\mathbf{s}$ and $\mathbf{u}$.

3.5.1 Formulating the optimization problem

Using the objective function given by equation (3.34) we can formulate the following optimization problem

$$\min_{\mathbf{s}\in\mathbb{R}^3,\mathbf{u}\in\mathbb{R}^{2n}} \mathbf{s}^T\mathbf{Q}\mathbf{s} + \sum_{k=1}^{l} \frac{1}{\mu_k} q_{G_k}^Q \tag{3.35a}$$

s.t

$$\mathbf{A}_{eq}\mathbf{x} - \mathbf{b}_{eq} = \mathbf{0} \tag{3.35b}$$

$$\mathbf{A}_{ineq}\mathbf{x} - \mathbf{b}_{ineq} \leq \mathbf{0} \tag{3.35c}$$

$$\sum_{i=1}^{n} f^L(\mathbf{u}_i) \leq p_{bus_j}^{avail} - p_{ext_j} \tag{3.35d}$$

The constraints in this problem are the same as in problem (3.19). Constraint (3.35b) is related to making sure that $\boldsymbol{\tau}$ is as close to $\boldsymbol{\tau_c}$ as possible. Constraint (3.35c) keeps the thrusters within their physical limitations, and constraint (3.35d) is there to make sure that the thrusters does not consume more power than what is available on the bus. By using equation (3.30), we can formulate an expression for $p_{bus_j}^{avail}$ as a function of the generators connected to the bus, given by equation (3.36).

$$p_{bus_j}^{avail} = \sum_{k=1}^{l} \mathbf{E}_{kj} p_{G_k}^{max} \tag{3.36}$$

$p_{G_k}^{max}$ is the maximum power generator number k can generate as given by its manufacturing specifications, and l is the total number of generators.

Problem (3.35) is formulated as a QP-problem, with an objective funtction that is quadratic in the decision variables defined as $\mathbf{s}$ and $\mathbf{u}$, and constraints which are linear in the decision variables. This problem will minimize the sum of the total fuel consumed by all the generators, while still making sure that $\boldsymbol{\tau}$ is as close to $\boldsymbol{\tau_c}$ as possible, the thrusters stay within their physical limitations and the thrusters does not consume more power than what is available on the bus that they are connected to.

3.6 Reducing generator load variations

Thrust allocation algorithms that helps with reducing load variations on the bus, are discussed in [Veksler et al., 2012a] and [Veksler et al., 2012b]. They introduce a term in the objective function, which relates a cost to the power consumed by the thrusters not being equal in the opposite direction of the change in the external power on the bus. This together with the fact that they allow for deviations from the DP-command $\boldsymbol{\tau_c}$, will make the thrusters counteract the load variations on the bus made by external equipment.

First of, reducing load variations on the bus by the use of thrusters means that the mean load on the bus will be higher. If load variations are not reduced, the generators will accelerate and de-accelerate which will lead to periods of incomplete combustion, followed by higher fuel consumption and soot formation. The mean temperature in the cylinders however, will be lower, meaning that NO_x production will be lower. Therefore the reduction of load variations can lead to an overall reduction in fuel consumption and soot formation, whereas NO_x production increases. In [Realfsen, 2009] they discuss the necessity of the generators working above a load of 25%-30% in order for cleaning by the Selective Catalytic Reduction (SCR)-filter of NO_x to be done. One could argue then, that if there are load variations on the bus that makes the generators vary around a load of 25%-30%, it would be beneficial for fuel consumption, soot formation and NO_x emissions to reduce the load variations, by increasing the mean load on the bus.

What we want to reduce are the variations in the load produced by the generators. This means that for generator k, we want $\dot{p}_{G_k}$ to be as small as possible. In order to minimize $\dot{p}_{G_k}$ for every k, we could introduce the term

$$\sum_{k=1}^{l} \frac{1}{\rho_k} \dot{p}_{G_k}^2 \tag{3.37}$$

where ρ_k is a weighting factor. Equation (3.37) is quadratic in the rate of change in generator load. The generator load is linear with respect to the thruster power and thruster power is approximated quadratically in thrust by $p_{T_i}^Q$ as shown in section 3.4. This means that equation (3.37) is not quadratic in the decision variables. In order to make it quadratic in the decision variables the thrust to power relationship of a thrusters can be linearised in each time-step by the same

procedure as in section 3.4.

$$\begin{aligned} p_{T_i} &= T_i^{3/2} \\ &= \sqrt{u_{i,surge}^2 + u_{i,sway}^2}^{3/2} \\ &= (u_{i,surge}^2 + u_{i,sway}^2)^{3/4} \\ &= (\mathbf{u}_i^T \mathbf{u}_i)^{3/4} \\ &\approx \frac{3 \cdot \mathbf{u}_{i,prev}^T}{2(\mathbf{u}_{i,prev}^T \mathbf{u}_{i,prev})^{1/4}} \mathbf{u}_i - \frac{(\mathbf{u}_{i,prev}^T \mathbf{u}_{i,prev})^{3/4}}{2} \\ &= p_{T_i}^L \end{aligned} \tag{3.38}$$

where $p_{T_i}^L$ is the linearization of p_{T_i} around the thrust values from the previous time-step $\mathbf{u}_{i,prev}$.

By using (3.32) we can replace $p_{T_i}^Q$ with $p_{T_i}^L$ and get

$$p_{G_k} = \sum_{j=1}^{m} \sum_{i=1}^{n} (\mathbf{E}^{-1})_{kj} \mathbf{M}_{ji} p_{T_i}^L + p_{ext_j} \tag{3.39}$$

Equation (3.39) is now a linear equation in the decision variables, that describes how much load generator k generates. If we insert equation (3.39) into equation (3.37) we get a quadratic function of the decision variables, which we can use to obtain the following cost function

$$J = \mathbf{s}^T \mathbf{Q} \mathbf{s} + \sum_{k=1}^{l} \frac{1}{\rho_k} \dot{p}_{G_k}^2$$

using Euler-discretization gives

$$J = \mathbf{s}^T \mathbf{Q} \mathbf{s} + \sum_{k=1}^{l} \frac{1}{\rho_k} \left(\frac{p_{G_k} - p_{G_{k,prev}}}{\Delta T} \right)^2 \tag{3.40}$$

where ΔT is the sample time of the thrust allocation. $p_{G_{k,prev}}$ is the produced power from the previous time-step, while p_{G_k} is calculated from equation (3.39).

3.6.1 Formulating the optimization problem

Using the objective function shown in equation (3.40) we can formulate optimization problem (3.41).

$$\min_{\mathbf{s}\in\mathbb{R}^3,\mathbf{u}\in\mathbb{R}^{2n}} \quad \mathbf{s}^T\mathbf{Q}\mathbf{s}+\sum_{k=1}^{l}\frac{1}{\rho_k}\left(\frac{p_{G_k}-p_{G_{k,prev}}}{\Delta T}\right)^2+\sum_{k=1}^{l}\frac{1}{\mu_k}q_{G_k}^Q \tag{3.41a}$$

$$\text{s.t}$$

$$\mathbf{A}_{eq}\mathbf{x}-\mathbf{b}_{eq}=\mathbf{0} \tag{3.41b}$$

$$\mathbf{A}_{ineq}\mathbf{x}-\mathbf{b}_{ineq}\leq\mathbf{0} \tag{3.41c}$$

$$\sum_{i=1}^{n}f^L(\mathbf{u}_i)\leq p_{bus_j}^{avail}-p_{ext_j} \tag{3.41d}$$

The third term in the objective function (3.41a) is introduced to ensure that when there are zero load variations on the bus, the thrust allocation problem should find the most fuel-efficient solution. When reduction of load variations are the main objective the second term in (3.41a) should be weighted higher than the third term. However, as always, $\mathbf{Q}$ should be weighted much higher than all the other terms in the objective function since $(\mathbf{s}\approx 0) \implies (\boldsymbol{\tau}\approx\boldsymbol{\tau_c})$.

Problem (3.41), in the case that variations in produced power on the generators are present, will seek to use the thrusters in such a way that these variations are reduced. If there are no variations in the produced power on the generators, fuel consumption will be minimized. Constraint (3.41b) is the constraint on the DP-command $\boldsymbol{\tau_c}$, constraints (3.41c) are the physical constraints on each thruster while constraint (3.41d) makes sure the thrusters does not consume more power than what is available on the bus.

3.7 Power reservation on the bus

In some cases there might be desirable to reserve power on the bus. When planning to switch on large external consumers, one could manually tell the thrust allocation algorithm beforehand, that a certain amount of power on one of the busbars, is reserved for an external consumer that is about to connect to the bus. One might envision this as an automated process as well, where an external consumer about to connect to the bus, tells the thrust allocation

how much power it needs. The thrust allocation can then reallocate thrust, and "make room" for the external consumer about to connect.

In the thrust allocation problem, power reservation can be handled with a constraint. When an external consumer is about to connect to the bus, it asks for power to be reserved, and the amount of power the thrusters can consume will be constrained as shown in equation (3.42).

$$\sum_{i=1}^{n} f^L(\mathbf{u}_i) \leq p_{bus_j}^{avail} - (p_{ext_j} + p_{res_j}) \tag{3.42}$$

p_{res_j} is the reserved power on bus number j, and $f^L(\mathbf{u}_i)$ is the linear function in the decision variables describing the power consumption of thruster number i. This constraint will reserve power on the bus for the equipment about to connect. As soon as the equipment that asked for reservation is connected, p_{res_j} is added to p_{ext_j} before p_{res_j} is set to zero. Equation 3.42 can be used as a constraint in any of the optimization problems presented in this thesis.

By reserving power for external consumers about to connect, by reallocating thrust one might prevent start up of extra generators. If the external consumer connects to the bus without power reservation, the PMS will start up additional generators to handle the oncoming load, if there is currently not enough available on the respective bus. Reducing the total amount of online generators will ultimately reduce the total fuel consumption of the power plant.

3.8 Sector constraints

In practice the thrusters cannot exert forces in any given direction, because they might flush other thrusters, disturb moonpool equipment, ROVs, divers etc. Figure 3.5 illustrates the concept of these forbidden sectors. Sector constraints has to be considered when formulating the optimization problem. However, these types of constraints are not considered in this thesis. In [Ruth, 2008] there is explained how these constraints can to be handled in the optimization problem. The problem that arises when introducing sector constraints is that the problem is no longer convex. This is usually solved by dividing each thrust-sector into several convex sectors and formulate convex sub QP-problems which can be solved efficiently. Each sub problem is a combination of allowed convex sectors, and each sub problem is solved as a QP-problem. The sub problem which has the lowest cost contains the thrust-sectors that should be used. Usually a supervisory controller is introduced to handle the switching between the different sub

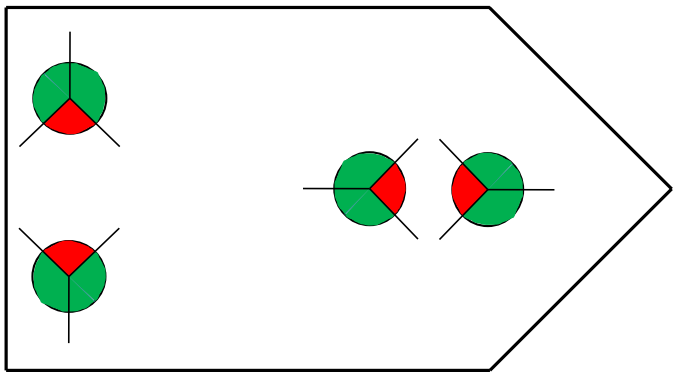

Figure 3.5: Illustration of forbidden sectors for any given thruster in red, and allowed sectors in green. This vessel is equipped with 4 azimuths, and the forbidden zones are such that the thrusters don't flush eachother. The allowed sectors(green) has to be divided into two sectors in order to get two convex sectors

problems. The supervisory controller switches from one sub problem to another based on at least two parameters; the cost function value of each sub problem and dwell time. The cost related to each sub problem is quite obvious; the sub problem with the lowest cost is favourable. But in order to avoid switching between two sub problems every other time-step, the supervisory controller also checks on the time since the last switch, this is called the dwell time. If the time since the last switch is greater than the dwell time and the cost is significantly lowered, the supervisory controller switches the sub problem to be used. One should also choose the convex allowed sectors such that they overlap, in order to avoid unnecessary switching.

To reiterate, these constraints are not considered in the problems formulated in this thesis and the reader is directed to [Ruth, 2008], [Larsen, 2012] and reference therein for more information on this subject. Some general information on these constraints are discussed however, because they need to be considered in any practical application. All the problems stated in this thesis can be modified to allow for sector constraints.

3.9 Single point of failure

In DP-class 2 and 3 there is a so called single point of failure requirement put forward by the classification societies. This means that a failure in one of the main components of the DP system, should not compromise the DP-capability of the vessel. This could be a failure in the position reference system; one of the thrusters; a generator; or even the loss of an entire main switchboard. Because of these requirements all DP-class 2 and 3 vessels has to be redundant in the technical design. In DP-class 2 the redundancy requirements are usually maintained by equipping the vessel with twice as many components as strictly necessary. DP-class 3 vessels are equipped in the same way as DP-class 2 vessels, but with an additional independent DP control system which is physically separated from the other redundant DP control systems, with fire- and waterproof bulkheads (A-60 class division) [DNV, 2011].

Because of the single point of failure requirements, the thrust allocation algorithm should handle failures in thrusters, generators and main switchboards in the sense that the optimization problem should still have a feasible solution.

In the case of failure in thruster number j, $T_{j,max}$ and $T_{j,min}$ in (3.17) can be set to zero. The thruster angle $\alpha_{j,max}$ and $\alpha_{j,min}$ can be set equal to $\alpha_{j,0}$. This will make the thruster stop at its current direction with zero thrust. If

there is a failure in one of the generators, the **E** matrix in equation (3.30) that decides the load sharing and amount of load each generator needs to generate, will have to be updated accordingly.

In addition to the thrust allocation being able to handle failure in relevant equipment, the classification societies requires an additional system to help prevent such failures to cause loss of heading and position. This is a so called "DP consequence analysis" which does online calculations every 5 minutes, according to classification requirements, that checks if there is enough generator capacity available if a worst-case single point failure should occur. These requirements are mostly for DP-class 2 and 3, where loss of position and heading are not acceptable because the vessels operate in very critical DP-operations. DP-class 0 and 1 vessels can accept loss of position and heading, and therefore the requirements on both software and technical design are less strict.

CHAPTER 4

Simulations and results

This chapter will present results from several simulations of the problems presented in chapter 3. As mentioned initially in this thesis, the dynamics of the vessel will not be considered, and it is assumed that as long as the DP-command $\boldsymbol{\tau_c}$ is obtained by the thrust allocation algorithm, the vessel will maintain its position and heading reference. Even though the vessel dynamics are not considered, the thruster-, generator- and busbar layout of the simulated vessel is needed. The dimensions for all the equipment are also needed in order to get simulations with realistic values. In this thesis the specification for the PSV Bourbon Tampen will be used in the simulations. Bourbon Tampen specifications are described in section 4.1 and B.

The simulations will show how the fuel minimizing optimization problem in section 3.5 performs with respect to more common thrust allocation methods like minimizing thrust, and power consumed by thrusters. There will also be shown that the fuel minimizing thrust allocation method can handle single point of failure in important equipment and worst case single point of failure on Bourbon Tampen. In order to reduce the number of plots, there will be no plot showing the produced generalized force $\boldsymbol{\tau}$ against the DP-command $\boldsymbol{\tau_c}$. Unless specified, the thrust allocation will produce the generalized forces given by $\boldsymbol{\tau_c}$. However, the numerical values for $\boldsymbol{\tau_c}$ used to generate the plots will be specified in each

figure and the values are given in kN.

The performance of the optimization problem in section 3.6 which is supposed to reduce load variations will also be presented. The implications of reducing load variations on fuel consumption and emission will be discussed.

The discussion will be had along with the presentation of each simulation and result, and all simulations will be done over 200 seconds where the thrust allocation algorithm is executed every second.

4.1 Bourbon Tampen

All the simulations in this thesis has been based on the specification of the PSV Bourbon Tampen whose technical specifications can be seen in appendix B, and the thought layout of all the relevant equipment can be seen in figure 4.1. There is 1 tunnel thruster and 1 azimuth thruster in front, and two azimuth thrusters aft which are used both in transit and in DP-operations. There are 4 diesel generators supplying all the equipment on board. There are two main busbars, with two generators connected to each one, with a bus-tie breaker between them. As mentioned earlier, this thesis assumes open bus-tie breaker in all operations/simulations. How all the equipment is assumed connected together can be seen in figure 4.1.

Since Bourbon Tampen is a DP-class 2 vessel which can be seen from its specification in appendix B under *classification*, all the simulations shown in this chapter will be most relevant for vessels of the same DP-class. Also make note that the worst-case single point failure for Bourbon Tampen will be the loss off an entire bus bar. The thrust allocation algorithm should therefore be able to produce feasible solutions in this situation.

4.2 Minimizing Thrust vs Minimizing Fuel

In this section there are presented simulations which compares problem (3.35) to problem (3.19). Problem (3.35) minimizes fuel while problem (3.19) minimizes thrust. In the objective function of problem (3.19) there is a $\mathbf{W}$ matrix where

$$\mathbf{W} = \begin{pmatrix} \mathbf{G} & \mathbf{0} \\ \mathbf{0} & \mathbf{Q} \end{pmatrix}$$

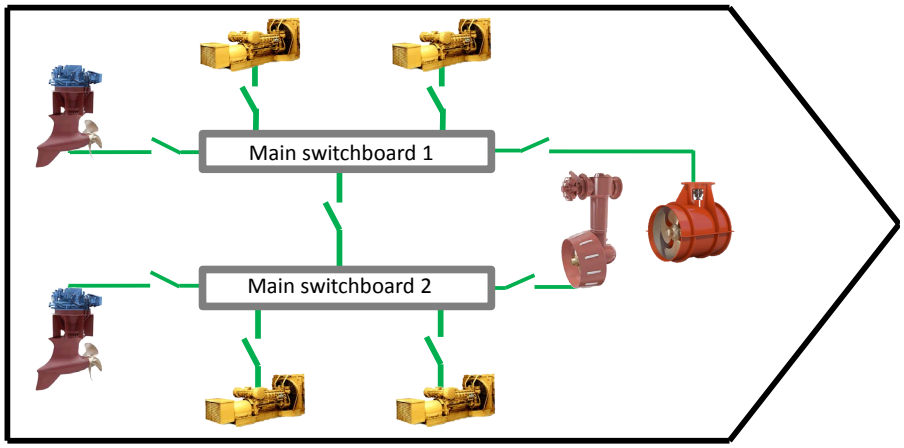

Figure 4.1: Illustration of the generator-, busbar- and thruster layout on Bourbon Tampen, and how they are assumed connected together

and **G** is a square diagonal matrix with weightings on each thruster. In this section there are shown simulations with two ways of choosing the weights in **G**. The first method set the weights on the diagonal equal to the inverse of each thrusters maximum thrust capacity, while the second approach is to set the weights on the diagonal of **G** equal for all thrusters. The first method will prefer solutions where the thrusters produce percentage wise equal amounts of thrust, while the second method will prefer solutions where the sum of total thrust is as small as possible.

In figure 4.2 the weights in **G** are set to the inverse of each thrusters maximum thrust capacity, and we see that after 100 seconds when the switch from thrust minimization to fuel minimization is done, that the generators consume less fuel and that the thrusters consume a little less power. In figure 4.4 the weights in **G** are equal for each thrusters. We see here that when the switch from thrust minimization to fuel minimization is done at 100 seconds, the fuel and power consumption stay constant. This is because there are no external load present on any of the buses, and it makes intuitive sense then, that when the total sum of thrust is minimized, power consumed by thrusters are minimized and fuel is minimized.

In figure 4.3 the weights in **G** are set to the inverse of each thrusters maximum thrust capacity again, the DP-command is changed slightly and a large external load are connected to the port bus bar. Not surprisingly, just as in figure 4.2 when the switch from thrust minimization to fuel minimization is done at 100 seconds, the fuel consumption by the generators and the power consumption of the thrusters both drop. In figure 4.5 the weights in **G** are equal for each thruster and the DP-command and external load are equal to the situation in figure 4.3. After 100 seconds when the switch from thrust minimization to fuel minimization is done, we notice that the fuel consumption drops and that the power consumption actually increases.

Some concluding remarks to these simulations and results is that the fuel minimizing thrust allocator will always produce solutions that uses less fuel than the thrust minimizing thrust allocator, except in special situations where there are no external load, and the weights in **G** are equal for every thruster, independent of its size. In these situations the fuel minimizing- and thrust minimizing thrust allocator will produce solutions that has the generators consume the same amount of fuel.

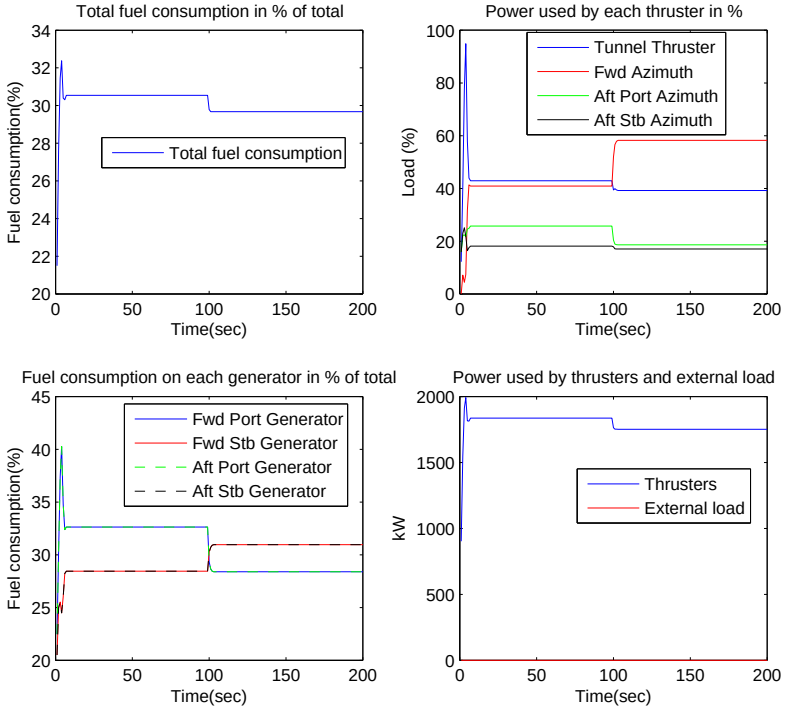

Figure 4.2: This simulation is done with $\boldsymbol{\tau_c} = \begin{pmatrix} 100 & 200 & 0 \end{pmatrix}^T$ and zero external load. In the first 100 seconds Thrust is minimized, and after 100 seconds fuel is minimized. When thrust is minimized the weights on the diagonal in the $\mathbf{G}$-matrix are the inverse of each thrusters maximum thrust capacity. $\sim 1\%$ fuel consumption reduction

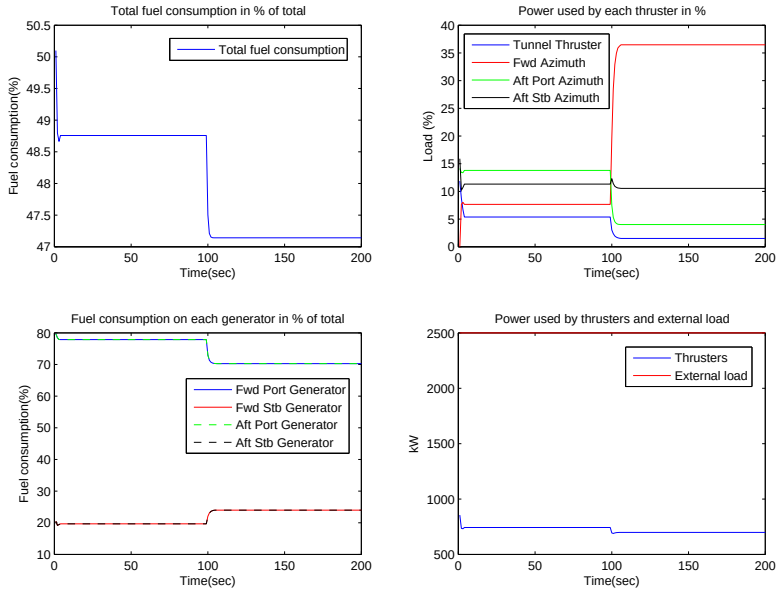

Figure 4.3: This simulation is done with $\boldsymbol{\tau_c} = \begin{pmatrix} 100 & 50 & 0 \end{pmatrix}^T$ and 2500kW of external load on the port busbar. In the first 100 seconds Thrust is minimized, and after 100 seconds fuel is minimized. When thrust is minimized the weights on the diagonal in the $\mathbf{G}$-matrix are the inverse of each thrusters maximum thrust capacity. $\sim 2\%$ fuel consumption reduction

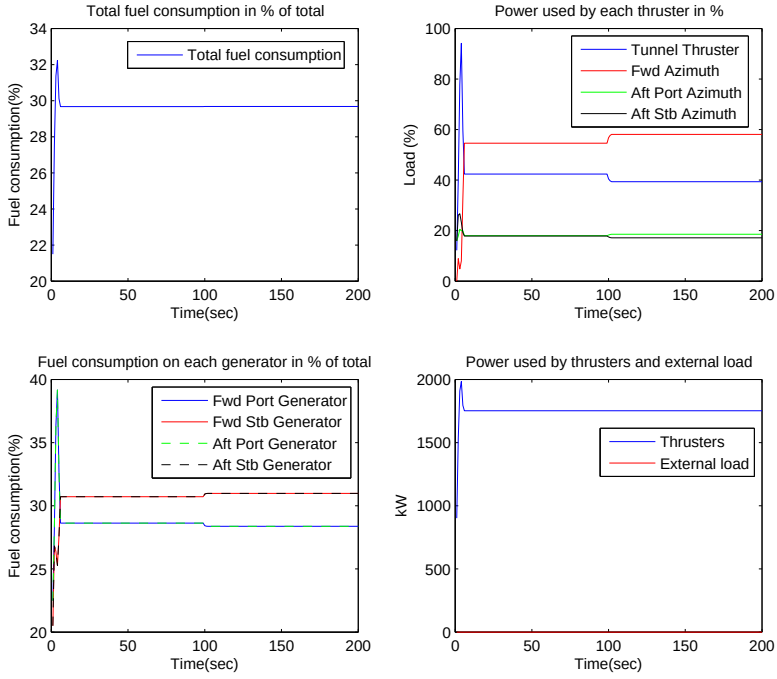

Figure 4.4: This simulation is done with $\boldsymbol{\tau_c} = \begin{pmatrix} 100 & 200 & 0 \end{pmatrix}^T$ and zero external load. In the first 100 seconds thrust is minimized, and after 100 seconds fuel is minimized. When thrust is minimized the weights on the diagonal of $\mathbf{G}$ are equal for all the thrusters. $\sim 0\%$ fuel consumption reduction

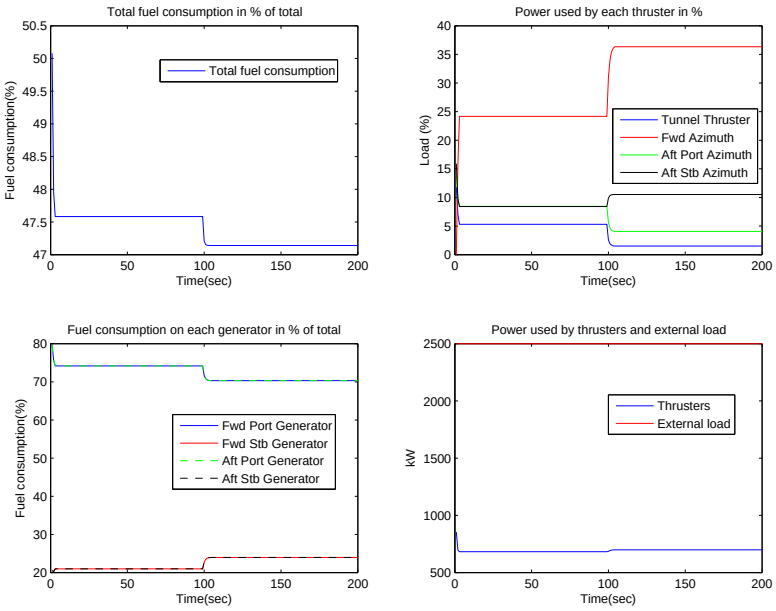

Figure 4.5: This simulation is done with $\boldsymbol{\tau_c} = \begin{pmatrix} 100 & 50 & 0 \end{pmatrix}^T$ and 2500kW of external load on the port busbar. In the first 100 seconds Thrust is minimized, and after 100 seconds fuel is minimized. When thrust is minimized the weights on the diagonal of $\mathbf{G}$ are equal for all the thrusters. $\sim 0.5\%$ fuel consumption reduction

4.3 Minimizing Power vs Minimizing Fuel

In this section, problem (3.35) is compared to problem (3.29) with a handful of simulations. The constraints are the same in both problems and they are the constraint related to obtaining the DP-command, physical max/min and rate constraints on thrusters and constraints that makes sure the thrusters does not consume more power than available on the bus. The objective functions differ however, and are repeated here for convenience.

$$J_1 = \mathbf{s}^T \mathbf{Q} \mathbf{s} + \sum_{k=1}^{l} \frac{1}{\mu_k} q_{G_k}^Q \tag{4.1}$$

$$J_2 = \mathbf{s}^T \mathbf{Q} \mathbf{s} + \sum_{i=1}^{n} \frac{1}{\gamma_i} p_{T_i}^Q \tag{4.2}$$

J_1 is the objective function in the fuel minimizing problem, while J_2 is the objective function in the power minimizing problem.

In all the simulations the second term in J_1 that puts a penalty on the use of fuel, is scaled such that it gives a cost between 0-100, and the generators are all penalised equally.

The second term in J_2 that puts a penalty on the power consumed by the thrusters are simulated with two different methods of scaling. One method sets γ_i equal to the maximum power consumption of thruster number i. This will make the thrusters consume power equally in percentage of their maximum capacity. The second method sets $\frac{1}{\gamma_i}$ outside the summation and $\gamma_i = \gamma$ equal to the maximum power consumption of all the thrusters combined. This will result in absolute minimum power consumption by the thrusters. In the simulations the second term in J_2 is also scaled such that it returns values between 0-100.

We notice from the results shown in figure 4.6 that after 100 second when the objective function switch from power minimization to fuel minimization is made, that indeed the generators consume less fuel. We also notice that the sum of power consumed by thrusters gets smaller. At first glance this might seem odd, since power was minimized the first 100 seconds. However, because of the scaling of the second term in J_2, the total sum of consumed power by the thrusters is not what is minimized. The scaling of the second term in J_2 prefers the thrusters to consume percentage wise equal amounts of power. This

can be seen in the top-right plot of figure 4.6 where in the first 100 seconds the thrusters work more equally, whereas in the last 100 seconds they separate more.

The comparison of the fuel minimizing objective function, with the power minimizing objective function that has this kind of scaling is included in this thesis, because it is a very common way to scale the second term in J_2.

If we change the scaling of the second term in J_2 such that the sum of total consumed power is minimized, we get the result shown in figure 4.7. And not surprisingly, both the fuel consumption of the generators and power consumption of the thrusters stay constant throughout the simulation. The objective functions switch at 100 seconds from power minimization to fuel minimization. We notice that the fuel consumption of each generator and the power consumption by each thruster changes slightly when the objective function changes. This does have an effect on the total fuel consumption, but it is so small that it cannot be seen in this plot.

From the results shown in figure 4.7 one might think that if one minimizes the sum of consumed power by all the thrusters, the fuel consumption will be minimized as well. This however, may not be the case if there are non-zero external consumers on the buses.

In figure 4.8 and figure 4.9 there is an external load on the port bus of 2500kW. Figure 4.8 has the same scaling of the second term in J_2 as the simulations shown in figure 4.6. As expected both the fuel and power consumption goes down in this simulation. In figure 4.9 however, we notice something interesting. The fuel consumption goes down, as expected but the total power consumed by the thruster actually increases. This is because of the external load that is present on the port busbar and the non-linear relationships between thrust, power and fuel. The non-linear relationship between fuel and power production of a generator dictates that the generator gets more efficient at high loads. When an external load is present on one busbar, the generators connected to this busbar gets a high load, while the generators connected to the busbar with no external load gets a low load in comparison. Transferring some of the thruster load from one busbar to the other, will therefore increase the overall efficiency of the power plant, and decrease the total fuel consumption. Because of the non-linear relationship between thrust and power, the total power consumption of the thrusters will increase. This is what we see from the plots in figure 4.9 and figure 4.8.

The concluding remarks of these simulations are pretty much the same as that in section 4.2. The fuel minimizing thrust allocation will always find solutions that uses less fuel than the power minimizing thrust allocation, except

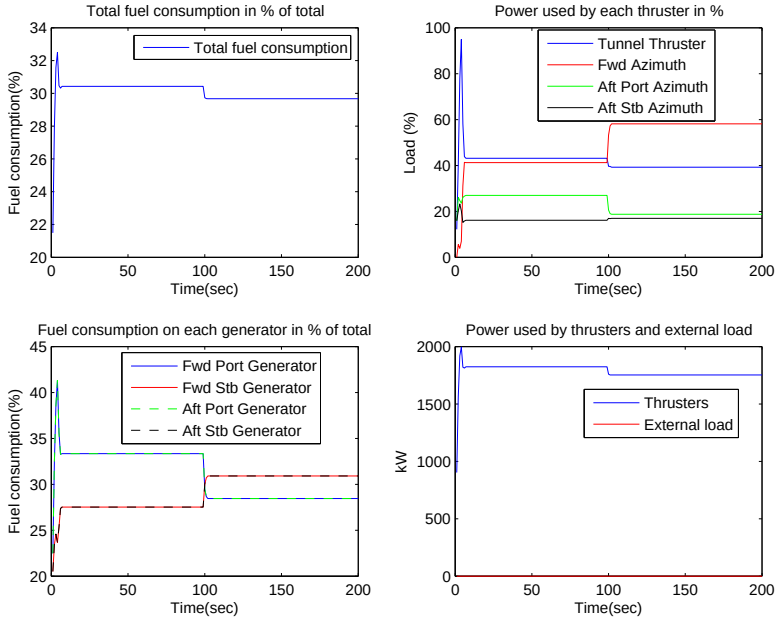

Figure 4.6: This simulation is done with $\boldsymbol{\tau_c} = \begin{pmatrix} 100 & 200 & 0 \end{pmatrix}^T$ and zero external load. Power consumed by the thrusters is minimized in the first 100 seconds while the last 100 seconds fuel consumption by the generators is minimized. In the first 100 seconds, power consumed by thruster number j is penalised with the inverse of its maximum possible power consumption. $\sim 1\%$ fuel consumption reduction.

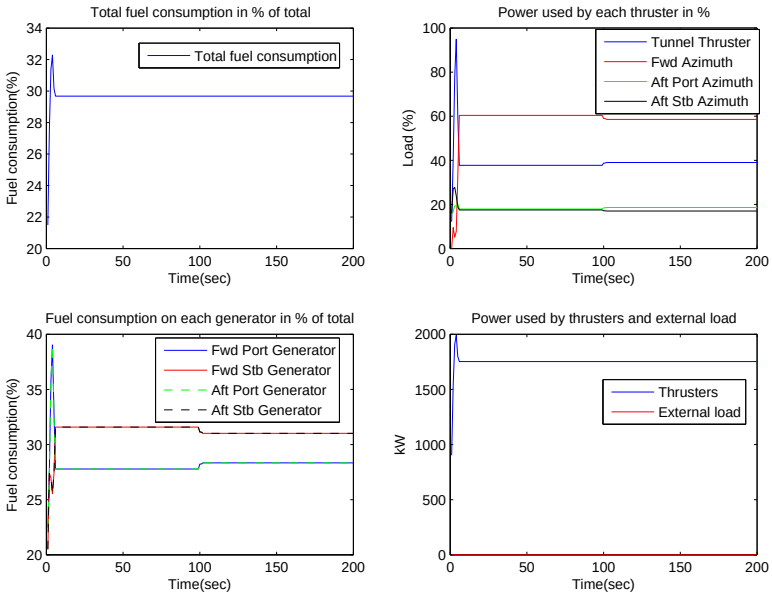

Figure 4.7: This simulation is done with $\boldsymbol{\tau_c} = \begin{pmatrix} 100 & 200 & 0 \end{pmatrix}^T$ and zero external load. Power consumed by the thrusters is minimized in the first 100 seconds while the last 100 seconds fuel consumption by the generators is minimized. In the first 100 seconds, the power consumption by each thruster is penalised independently of its size. $\sim 0\%$ fuel consumption reduction.

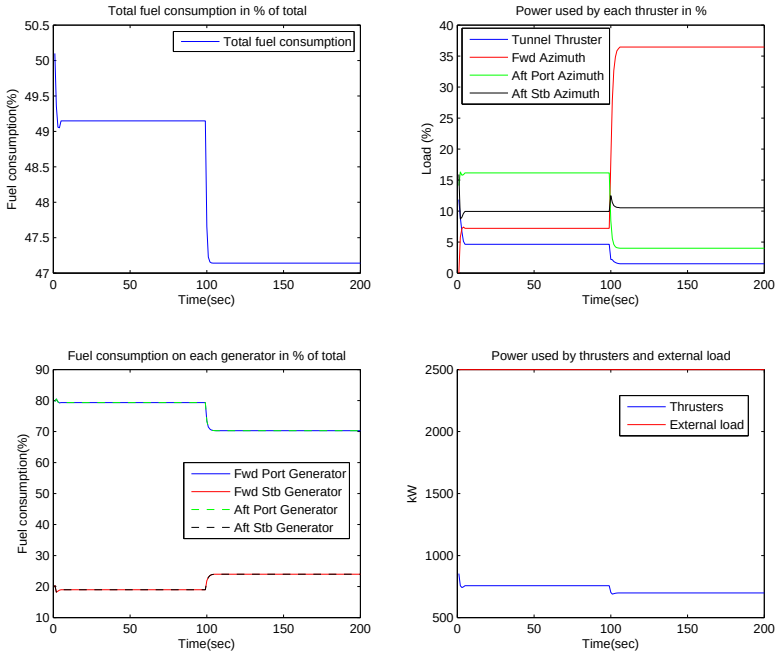

Figure 4.8: This simulation is done with $\boldsymbol{\tau_c} = \begin{pmatrix} 100 & 50 & 0 \end{pmatrix}^T$ external load of 2500kW on the port busbar. Power consumed by the thrusters is minimized in the first 100 seconds while in the last 100 seconds fuel consumption, by the generators is minimized. In the first 100 seconds, power consumed by thruster number j is penalised with the inverse of its maximum possible power consumption. $\sim 2\%$ fuel consumption reduction.

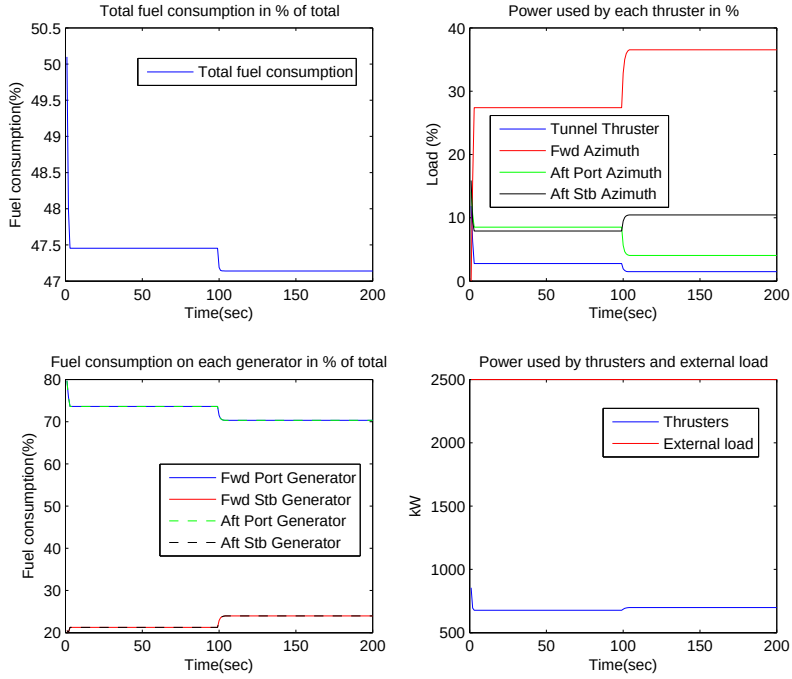

Figure 4.9: This simulation is done with $\boldsymbol{\tau_c} = \begin{pmatrix} 100 & 50 & 0 \end{pmatrix}^T$ external load of 2500kW on the port busbar. Power consumed by the thrusters is minimized in the first 100 seconds while the last 100 seconds fuel consumption by the generators is minimized. In the first 100 seconds, the power consumption by each thruster is penalised independently of its size. $\sim 1\%$ fuel consumption reduction. $\sim 0.5\%$ fuel consumption reduction.

in special situations where there are no external loads. If there are no external load, the fuel minimizing thrust allocation and the power minimizing thrust allocation will produce solutions that will consume the same amount of fuel. One could say that the fuel minimizing thrust allocation finds solutions that consumes less or equal amounts of fuel as both the thrust minimizing thrust allocation and the power minimizing thrust allocation.

4.4 Reducing Load Variations

In this section simulations of problem (3.41) are presented.

Figure 4.10 shows the result of a simulation over 200 seconds, where an external load is switched on after 20 seconds and oscillates around 1000kW with an amplitude of 100kW and a frequency of 0.08Hz. The first 100 seconds of the simulation is done with an objective function that minimizes power consumption of the thrusters, and we see that thrusters operate at a steady state, while the load on the generators oscillate proportionally to the external load variations. After 100 seconds, the objective function switches to the one in problem (3.41). We notice that the thrusters starts counteracting the varying external load on the bus, such that the generated load by the generators evens out.

The load variations on the generators are reduced as shown in figure 4.10. This will lead to less wear and tear on the generators, and will lead to smaller frequency variations on the bus, which if large enough, can cause a black-out. The trade off is that the wear and tear on the thrusters will increase which becomes evident by looking at the power consumed by the thrusters in figure 4.10.

How the fuel consumption behaves during the simulation can be seen in the top-left plot of figure 4.10. Since the fuel consumption is based on a static model, the fuel consumption in situations where the dynamics of the diesel generator is excited will not be correctly represented by the model in this thesis. In fact when load variations are present in the produced power of the generators, the fuel consumption is probably higher than the static model shows. The model is a good approximation for the fuel consumption in steady-state situations, or situations where the load varies slowly enough to not excite the dynamics and large transients behaviour in the generator.

In the bottom-left plot of figure 4.10 we notice that the generators connected to the bus with the oscillating external load also has oscillations in their load before the load reduction is switched on, which is expected of course. After

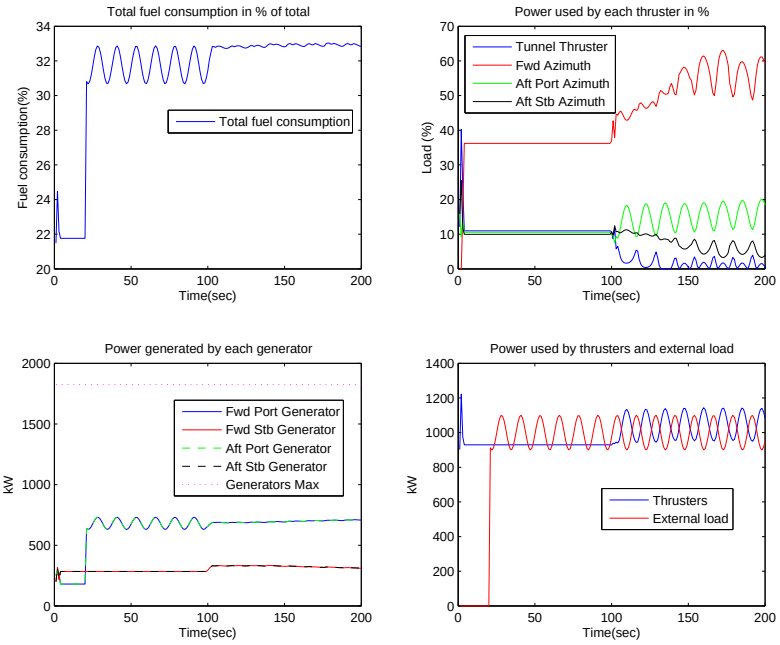

Figure 4.10: This simulation is done with $\boldsymbol{\tau_c} = \begin{pmatrix} 100 & 100 & 0 \end{pmatrix}^T$ and after 20 seconds an external load on the port bus bar that varies periodically around 1000kW with amplitude of 100kW and a frequency of 0.08Hz is switched on. The first 100 seconds of this simulation minimizes power consumed by the thrusters. After 100 seconds the objective function is switched to the one in problem (3.41) which penalises changes in the load on each generator from one time-step to the next

the load reduction is switched on, the oscillation on these generators are reduced significantly, while the load of the two other generators increase slightly. This means that the mean power produced by the generators are higher after the load variation reduction is switched on and lower before. As discussed in section 3.6, variations in the power produced by a generator will lead to periods of incomplete combustion which implies higher fuel consumption and more soot pollution. Also, the higher the mean load on the generators are, the less NO_x will be produced. So, in the situation before the load variation reduction is switched on, where we have load variations on the generators, the fuel consumption and soot formation will be high, while NO_x production will be low. After the load variation reduction is switched on however, the generators will operate with smaller load variations which implies lower fuel consumption and soot production, but since the mean load has to increase, NO_x production will increase as well. It was also discussed in section 3.6, that the generators had to work above a specific percentage of their maximum capacity, in order for cleaning of NO_x be done by an SCR-filter. One might find oneself in a situation then, where by reducing the load variations on the bus and increasing the mean load such that NO_x cleaning can be done, you will effectively reduce fuel consumption, sooting and NO_x emission.

4.5 Power Reservation on the Bus

In this section there is illustrated a scenario where the thrust allocation algorithm, if given the information, can "make room" on the bus for consumers about to connect to the bus by reserving power on the bus. How the thrust allocation algorithm could do this is explained in section 3.7, and the suggested method is by using equation (3.42) as a constraint in any of the optimization problems presented in this thesis.

In figure 4.11 a simulation of the power reservation is shown. One of the generators on the port side is disconnected from the bus, such that the available power on the port bus bar is lower than on the starboard side. In this simulation the power consumption on the port bus bar will saturate, and in this way the accuracy of the linearization of maximum available power shown by equation (3.28) in subsection 3.4.1 can also be tested.

The fuel minimizing optimization problem from section 3.5, where constraint (3.35d) is switched with equation (3.42), is used throughout the whole simulation. After 100 seconds an external consumer of 1000kW wishes to connect to

the port busbar, and it asks the thrust allocation algorithm to reserve 1000kW on the port bus bar so that it can connect. At 110 seconds the external consumer begins to connect, and it does so over a period of 4 seconds.

We notice at 100 seconds that when the reservation of 1000kW is made, the thrust allocates thrust such that the load on the port busbar reduces enough to make room for the external consumer about to connect. At 110 seconds the external consumer connects to the bus over a period of 4 seconds, and we notice that the thrusters can stay constant while the consumer connects. This reservation makes it possible to make sure that there will be enough available power on the bus before the external consumers connects, without the need to start the second generator. If the external consumer connected before the reservation, we see that there is not enough power available on the port bus, so the PMS might start up a new generator in order to make room for the external consumer about to connect. As we see, the second generator on the port bus is not necessary in this situation, and starting up more generators than necessary is never fuel efficient.

4.6 Single Point of Failure

All simulations in this section will be done with the fuel minimizing optimization problem from section 3.5. There will be shown a few scenarios where a failure in some of the relevant equipment(thrusters, generators and bus bars) occurs, to see if the fuel minimizing thrust allocation algorithm can handle it.

In figure 4.12 a simulation is shown, where after 100 seconds the forward azimuth thruster disconnects from the bus. The thrusters reallocate their forces in order to make sure that the DP-command $\boldsymbol{\tau_c}$ is still obtained, and we notice that the total fuel consumption actually increases. This shows that can be more fuel efficient to operate with more thrusters than necessary to obtain $\boldsymbol{\tau_c}$. This arises because of the non-linear relationship between fuel and produced power of a generator. When one thruster disconnects the remaining thrusters have to pick up the slack which leads to increased fuel consumption. When a thruster failure is present it is chosen to ”freeze” its direction, which can be seen in the lower right plot of figure 4.12.

Figure 4.13 is the same scenario as in figure 4.12 except that instead of a thruster failure at 100 seconds, the forward port generator disconnects from the bus. The thrusters changes their thrust and direction slightly, and not surprisingly we notice that the total fuel consumption goes down. This is because it

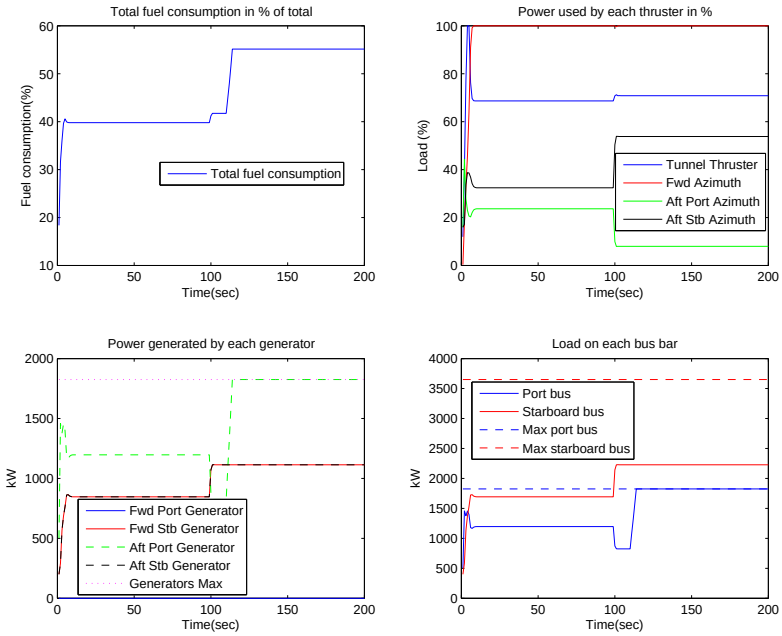

Figure 4.11: This simulation is done with $\boldsymbol{\tau_c} = \begin{pmatrix} 100 & 300 & 0 \end{pmatrix}^T$ and one of the generators on the port bus bar is disconnected. The fuel minimizing thrust allocator is used the whole simulation, and at 100 second 1000kW is reserved on the port bus bar. at 110 seconds the consumer that reserved the power connects to the bus over a period of 4 seconds.

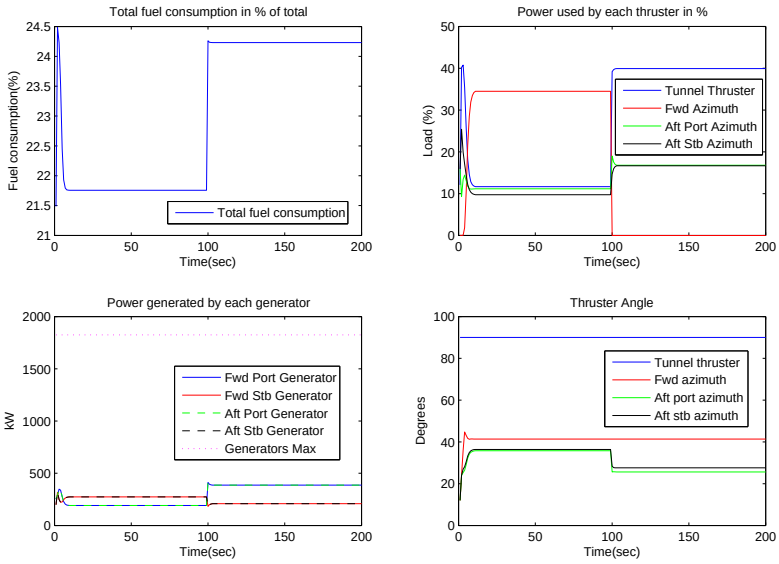

Figure 4.12: This simulation is done with $\boldsymbol{\tau_c} = \begin{pmatrix} 100 & 100 & 0 \end{pmatrix}^T$, and the fuel minimizing optimization problem is used throughout the simulation. After 100 seconds the forward azimuth thruster is disconnected from the bus.

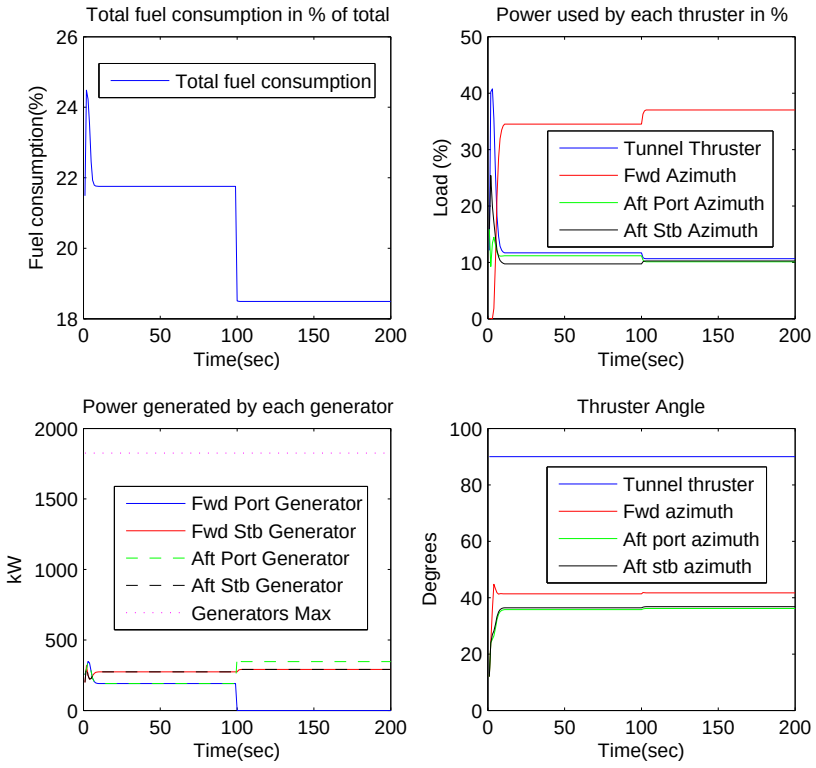

Figure 4.13: This simlation is done with $\boldsymbol{\tau_c} = \begin{pmatrix} 100 & 100 & 0 \end{pmatrix}^T$, and the fuel minimizing optimization problem is used throughout the simulation. After 100 second the forward port generator is disconnected from the bus.

is most fuel efficient to not operate with more online generators than necessary, and clearly it is not necessary to operate with all generators online in this simulation scenario.

The simulation scenario in figure 4.14 goes one step further and simulates a scenario called "worst-case single point failure". This is a situation where a short circuit occurs in one of the bus bars, which causes all the equipment connected to the bus bar to disconnect from the bus. This means that the vessel loses half of its thrusters, and half of its generators. Because Bourbon Tampen is a DP-class 2 vessel, it has redundancy in its technical design as required by classification societies which mean it should handle situations where one of the bus bars is lost. This is also discussed to some extent in section 3.9. By the results in figure 4.14, we notice that the thrust allocation handles the failure in both port generators and both thrusters connected to the port bus bar, that occurs after 100 seconds. The DP-command is not shown in order to save space, but it is obtained such that position and heading is never lost.

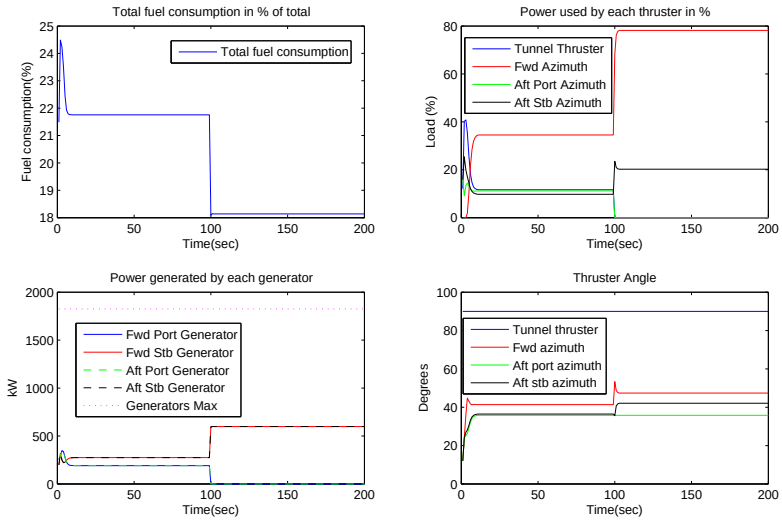

Figure 4.14: This simulation is done with $\boldsymbol{\tau_x} = \begin{pmatrix} 100 & 100 & 0 \end{pmatrix}^T$, and the fuel minimizing optimization problem is used throughout the simulation. After 100 seconds a short circuit in the port bus bar is simulated, leading to a black out of the bus bar.

CHAPTER 5

Conclusion

The main contribution of this thesis has been the development of a thrust allocation algorithm that incorporates the consumed fuel by the generators into the objective function. The fuel minimizing thrust allocation were developed by finding a static model of the fuel consumption of the generators, and known thruster models relating thrust to consumed power. Simulations showed that the fuel minimizing thrust allocation algorithm performs well, when compared to known thrust- and power minimizing thrust allocation algorithms.

As well as presenting simulations of the fuel minimizing thrust allocation compared to thrust- and power minimizing thrust allocators, other fuel- and emission related simulation scenarios has been presented. There has been presented a thrust allocation that penalises variations in the produced power of the generators, and it has been shown that it effectively reduces the load variations. The implications of reducing load variations has been discussed in section 3.6 and section 4.4, but the general conclusion is that it becomes a trade-off between two things. Not reducing load variations leads to wear and tear on the generators, higher fuel consumption and more sooting. Reducing the load variations will lead to more wear and tear on the thrusters and higher NO_x emission.

Additionally there has been presented a functionality that can make the thrust allocation algorithm reserve power on the bus. The simulations showed

that by reserving power on the bus for external consumers about to connect, one might avoid the need to start up additional generators to handle the consumers about to connect. Avoiding start up of more generators will always be more fuel efficient. It has also been shown that the fuel minimizing thrust allocation algorithm will handle single point of failure, and worst case single point of failure on Bourbon Tampen. During these simulations it was discovered that it can be more fuel efficient to operate with as many online thrusters as possible.

The fuel optimization can be implemented within the conventional framework of quadratic programming-based thrust allocation, by recalculating the cost function and constraints based on linear and quadratic model approximations at the current operation point.

Bibliography

[Ådnanes, 2003] Ådnanes, A. K. (2003). *Maritime electrical installations and diesel electric propulsion*. Fakultet for ingeniørvitenskap og teknologi, Norges teknisk-naturvitenskapelige universitet, Institutt for marin teknikk.

[Aithal, 2010] Aithal, S. (2010). Modeling of NOx formation in diesel engines using finite-rate chemical kinetics. *Applied Energy*, 87(7):2256–2265.

[Bodson, 2002] Bodson, M. (2002). Evaluation of optimization methods for control allocation. *Journal of Guidance, Control, and Dynamics*, 25(4):703–711.

[DieselServiceAndSupply, 2013] DieselServiceAndSupply (2013). Approximate fuel consumption chart. `http://www.dieselserviceandsupply.com/temp/Fuel_Consumption_Chart.pdf`. [Online; accessed 23-April-2013].

[DNV, 2011] DNV (2011). *Rules For Classification Of Ships. Dynamic Positioning Systems*. Det Norske Veritas.

[Fossen and Johansen, 2006] Fossen, T. and Johansen, T. (2006). A survey of control allocation methods for ships and underwater vehicles. In *Control and Automation, 2006. MED '06. 14th Mediterranean Conference on*, pages 1–6.

[Fossen, 2002] Fossen, T. I. (2002). *Marine Control Systems*. Marine Cybernetics.

[Garus, 2004] Garus, J. (2004). Optimization of thrust allocation in propulsion system of underwater vehicle. *International Journal of Applied Mathematics and Computer Science*, 14(4):461–467.

[Guzzella and Onder, 2010] Guzzella, L. and Onder, C. H. (2010). *Introduction to modeling and control of internal combustion engine systems*. Springer.

[Hansen, 2000] Hansen, J. F. (2000). Modeling and control of marine power systems. *Doctor thesis, Norwegian University of Science and Technology, Department of Engineering cybernetics, Trondheim, Norway*.

[Jenssen and Realfsen, 2006] Jenssen, N. A. and Realfsen, B. (2006). *Power Optimal Thruster Allocation*. MTS Dynamic Positioning Conference, Houston.

[Johansen et al., 2004] Johansen, T., Fossen, T., and Berge, S. (2004). Constrained nonlinear control allocation with singularity avoidance using sequential quadratic programming. *Control Systems Technology, IEEE Transactions on*, 12(1):211–216.

[Johansen and Fossen, 2013] Johansen, T. A. and Fossen, T. I. (2013). Control allocation-a survey. *Automatica*, 49:1087–1103.

[Johansen et al., 2005] Johansen, T. A., Fossen, T. I., and Tøndel, P. (2005). Efficient optimal constrained control allocation via multiparametric programming. *Journal of guidance, control, and dynamics*, 28(3):506–515.

[Johansen et al., 2003] Johansen, T. A., Fuglseth, T. P., Tøndel, P., and Fossen, T. I. (2003). *Optimal Constrained Control Allocation In Marine Surface Vessels With Rudders*. IFAC Conf. Manoeuvring and Control of Marine Craft, Girona.

[Kongsberg, 2012] Kongsberg (2012). Kongsberg maritime. `http://www.km.kongsberg.com`.

[Larsen, 2012] Larsen, K. E. (2012). *Fuel-Efficient Control Allocation for Supply Vessels*. Norwegian University of Science and Technology. M.Sc Thesis.

[Leavitt, 2008] Leavitt, J. (2008). Optimal thrust allocation in dp systems. Houston. L-3 Communications DPCS, MTS Dynamic Positioning Conference.

[Lindegaard and Fossen, 2003] Lindegaard, K.-P. and Fossen, T. I. (2003). Fuel-efficient rudder and propeller control allocation for marine craft: experiments with a model ship. *Control Systems Technology, IEEE Transactions on*, 11(6):850–862.

[Mathiesen et al., 2012] Mathiesen, E., Realfsen, B., and Breivik, M. (2012). *Methods for Reducing Frequency and Voltage Variations on DP Vessels*. MTS Dynamic Positioning Conference, Houston.

[Nocedal and Wright, 2006] Nocedal, J. and Wright, S. J. (2006). *Numerical Optimization, Second Edition*. Springer.

[Radan, 2008] Radan, D. (2008). *Integrated control of marine electrical power systems*. PhD thesis, Norwegian University of Science and Technology.

[Realfsen, 2009] Realfsen, B. (2009). *Reducing NOx Emission in DP2 and DP3 Operations*. MTS Dynamic Positioning Conference, Houston.

[Ruth, 2008] Ruth, E. (2008). *Propulsion control and thrust allocation on marine vessels*. Norwegian University of Science and Technology. Doctoral Thesis.

[Sørdalen, 1997] Sørdalen, O. (1997). Optimal thrust allocation for marine vessels. *Control Engineering Practice*, 5(9):1223–1231.

[Veksler et al., 2012a] Veksler, A., Johansen, T. A., and Skjetne, R. (2012a). Thrust allocation with power management functionality on dynamically positioned vessels. In *American Control Conference (ACC), 2012*, pages 1468–1475. IEEE.

[Veksler et al., 2012b] Veksler, A., Johansen, T. A., and Skjetne, R. (2012b). *Transient power control in dynamic positioning - governor feedforward and dynamic thrust allocation*. IFAC Conference on Manoeuvring and Control of Marine Craft, Arenzo.

[Widd, 2012] Widd, A. (2012). *Physical Modeling and Control of Low Temperature Combustion in Engines*. PhD thesis, Department of Automatic Control, Lund University, Sweden.

[Widd et al., 2009] Widd, A., Ekholm, K., Tunestal, P., and Johansson, R. (2009). Experimental evaluation of predictive combustion phasing control

in an hcci engine using fast thermal management and vva. In *Control Applications,(CCA) & Intelligent Control,(ISIC), 2009 IEEE*, pages 334–339. IEEE.

[Widd et al., 2008] Widd, A., Tunestal, P., and Johansson, R. (2008). Physical modeling and control of homogeneous charge compression ignition (hcci) engines. In *Decision and Control, 2008. CDC 2008. 47th IEEE Conference on*, pages 5615–5620. IEEE.

[Wikipedia, 2012] Wikipedia (2012). Dynamic positioning. `http://en.wikipedia.org/wiki/Dynamic_positioning`. [Online; accessed 12-September-2012].

[Wit, 2009] Wit, C. D. (2009). *Optimal Thrust Allocation Methods for Dynamic Positioning of Ships*. Delft University of Technology, Netherlands. M.Sc Thesis.

Appendices

APPENDIX A

Fuel Optimal Thrust Allocation in Dynamic Positioning - Paper

Fuel Optimal Thrust Allocation in Dynamic Positioning

Martin Rindaroey * **Tor Arne Johansen** *

* *Center for Autonomous Marine Operations and Systems, Department of Engineering Cybernetics, Norwegian University of Science and Technology, Trondheim, Norway. (e-mail: tor.arne.johansen@itk.ntnu.no)*

Abstract: This paper is focused on the thrust allocation algorithm, which is a part of a Dynamic Positioning (DP) system in marine vessels with diesel-electric power system. In this paper the focus will be on using the thrust allocation to make the diesel generators on board the vessel work more fuel efficiently, by reducing the total fuel consumption of all online diesel generators. A static model for the fuel consumption of a diesel generator as a function of its produced power will be derived from data, and this model will be used to create a convex Quadratic Programming (QP)-problem which finds the most fuel efficient thrust allocation solutions. The simulation scenarios shown in this paper typically gives a fuel reduction of a rather common Platform Supply Vessel (PSV) of up to 2% of its maximum possible fuel consumption. The fuel optimization can be implemented as a standard QP-problem by recalculation of its cost function weights based on linear and quadratic model approximations at the current operation point.

1. INTRODUCTION

In today's marine industry there are many operations e.g; pipelay operations, dredging, crane barge operations, station keeping, drilling, anchor handling etc, that are performed at low speeds and requires the vessel to maintain heading and/or position. In order to achieve this the vessel is equipped with thrusters such that longitudinal and latitudinal thrust forces can be produced at all times, and a DP system to control them.

The three main parts of the DP control system is a state estimator, a high-level motion controller and the thrust allocation algorithm. The high-level motion controller calculates forces in surge, sway and yaw needed to maintain position and heading, while the thrust allocation algorithm takes the vector containing these forces, and calculates thrust and direction for each active thruster. The thrust allocation algorithm is the focus of this paper.

The thrust allocation problem, because most DP vessels are over-actuated, is usually solved as an optimization problem, searching for solutions within the thrusters physical limitations, while minimizing some user-defined criterion. Thrust allocation has been an active area of research for the past two decades, and the criterion which is minimized are usually produced thrust or consumed power by the thrusters, while taking physical constraints like azimuth turn rate, forbidden zones, maximum thrust capacity etc. into account.

A paper which has a general view of the control allocation problem is Johansen and Fossen [2013]. They present constrained and unconstrained optimization problems to solve the allocation problem, and the criterion to be minimized is usually some penalty related to the use of actuators or violation of constraints.

Fossen and Johansen [2006] is a survey of control allocation methods for marine vessels. They introduce optimization problems which solves the thrust allocation problem with respect to physical constraints on the thrusters and a constraint which specifies that the DP-command should be obtained. The criterion which is minimized, is a penalty on slack variables on the DP-command constraint, since there might be situations where it is just not possible to obtain the DP commanded total thrust, and with a hard constraint in these situations the optimization problem would have no feasible solution. In addition to the slack variables, there are different criteria which also include either the produced thrust, or the consumed power by the thrusters. Thrust allocation algorithms that seek to minimize the consumed power of the thrusters are seen in e.g, Jenssen and Realfsen [2006],Leavitt [2008],Larsen [2012],Wit [2009], Ruth [2008],Veksler et al. [2012a],Johansen et al. [2004] and Veksler et al. [2012b].

Veksler et al. [2012b] and Veksler et al. [2012a] as well as minimizing consumed power by the thrusters, presents a method to reduce load variations on the bus by dynamically biasing the thrusters. Two methods for reducing frequency and load variations in the power distribution is also discussed in Mathiesen et al. [2012].

The authors have not found anything in the literature where the thrust allocation algorithm explicitly includes the fuel consumption of online diesel generators in the cost function. Instead, thrust allocation algorithms in the literature tend to minimize the power consumed by the thrusters and some take the load conditions on the bus into consideration. Radan [2008] and Hansen [2000], has some discussion on the fuel-optimal operation conditions of a diesel generator plant on a vessel, but they both discuss it from a Power Management System (PMS) point of view.

Aithal [2010],Widd [2012] and Guzzella and Onder [2010], to name a few, discuss diesel engines fuel consumption and emissions. The diesel generator models presented in Aithal [2010] and Widd [2012] seem however too complex to use in a thrust allocation algorithm.

This paper investigates the possibility to use the thrust allocation algorithm in such a way that the fuel consumption of the online diesel generators on each power bus will be minimized. A simple model of the fuel consumption of a diesel generator as a function of its produced power will be derived from sampled data, and incorporated in an optimization problem which will be used to solve the thrust allocation problem. The fuel consumption of the diesel generators on each power bus will be formulated as a quadratic function of produced thrust and minimized, while making sure that thrusters operate within their physical limitations and that the DP-command is obtained if possible. There will also be some discussion on the implication of variations in the produced power by a diesel generator and its fuel consumption, sooting and NO_x emission. The results are illustrated with DP class 2 operations of a typical PSV.

2. FORMULATING THE FUEL OPTIMAL THRUST ALLOCATION PROBLEM

The thrust allocation problem can be formulated as shown in the optimization problem (1), where all the variables and symbols used in this paper are described in Table 1.

$$\min_{\mathbf{u}\epsilon\mathbb{R}^{2n},\mathbf{s}\epsilon\mathbb{R}^3} \quad \mathbf{s}^T\mathbf{Q}\mathbf{s} + f(\cdot) \tag{1a}$$

s.t

$$\boldsymbol{\tau_c} - \mathbf{B}\mathbf{u} - \mathbf{s} = \mathbf{0} \tag{1b}$$

$$\mathbf{u}_{min} \leq \mathbf{u} \leq \mathbf{u}_{max} \tag{1c}$$

$$\boldsymbol{\Delta}\mathbf{u}_{min} \leq \boldsymbol{\Delta}\mathbf{u} \leq \boldsymbol{\Delta}\mathbf{u}_{max} \tag{1d}$$

$$\boldsymbol{\alpha}_{min} \leq \boldsymbol{\alpha} \leq \boldsymbol{\alpha}_{max} \tag{1e}$$

$$\boldsymbol{\Delta\alpha}_{min} \leq \boldsymbol{\Delta\alpha} \leq \boldsymbol{\Delta\alpha}_{max} \tag{1f}$$

$$\sum_{i=1}^{n} \mathbf{M}_{ji} p_{T_i} \leq p_{bus_j}^{avail} - p_{ext_j} \quad \forall j \in \{1, 2, \ldots, m\} \tag{1g}$$

This problem will minimize the slack variables $\mathbf{s}$ while making sure that constraint (1b) is satisfied, meaning the DP-command is obtained if possible, and the thrusters operate within their physical limitations by constraint (1c)-(1f). Constraint (1g) makes sure the thrusters does not consume more power than available on the bus.

Since the thrust allocation problem is usually over-actuated, there usually exists many solutions that satisfies the constraints given by (1b)-(1g). This gives us some freedom in choosing which of the solutions we would prefer, and we do this with the help of the function $f(\cdot)$ in (1a). In this paper $f(\cdot)$ will primarily be used to describe the fuel consumed by the online generators. This will lead to thrust allocation solutions that tries to have the generators consume as little fuel as possible while satisfying constraints.

It is beneficial if the thrust allocation problem can be formulated as a convex QP-problem, since these are well known and relatively easy to solve numerically. This implies that constraints (1c)-(1g) have to be linear, and they can be found in the literature, e.g Larsen [2012] and Ruth [2008]. In addition to linear constraints, a QP-problem also needs a convex quadratic objective function. This means that when designing $f(\cdot)$ it has to be quadratic and convex in the decision variables given by $\mathbf{u}$.

Letter	*Description*
$\mathbf{s}$	Slack variables that relaxes constraint (1b). This is the constraint which specifies that the thrusters should obtain the DP-command given by $\boldsymbol{\tau_c}$
$\mathbf{u}$	Vector containing each thrusters forces in both surge and sway direction. $\mathbf{u} = \begin{pmatrix}\mathbf{u}_1 & \mathbf{u}_2 & \ldots & \mathbf{u}_{2n}\end{pmatrix}^T$, $\mathbf{u}_i = \begin{pmatrix}u_{i,surge} & u_{i,sway}\end{pmatrix}^T$
$\boldsymbol{\Delta}\mathbf{u}$	Change in thrust from one time-step to the next
$\boldsymbol{\Delta}\mathbf{u}_{min}/\boldsymbol{\Delta}\mathbf{u}_{max}$	Maximum allowed thrust reduction/increase from on time-step to the next.
$\boldsymbol{\alpha}$	Azimuth direction, given by $atan2\left(u_{i,sway}, u_{i,surge}\right)$ for thruster number i
$\boldsymbol{\Delta\alpha}$	Change in thrust direction from one time-step to the next
$\boldsymbol{\Delta\alpha}_{min}/\boldsymbol{\Delta\alpha}_{max}$	Maximum allowed thrust angle reduction/increase from one time-step to the next.
$\mathbf{Q}$	Symmetric positive weighting matrix, used to put a cost on the use of slack variables $\mathbf{s}$. Reducing the values of the slack variables has the highest priority, so the weights in $\mathbf{Q}$ should be such that the cost of the first term in (1a) is larger than the second term.
$\mathbf{B}$	Control allocation matrix. Maps the $2n$ dimensional thrust vector $\mathbf{u}$, to the 3 dimensional $\boldsymbol{\tau}$-vector.
$\mathbf{M}$	$m \times n$ matrix with 1's and 0's stating which thruster is connected to which bus.
$\mathbf{E}$	$l \times l$ matrix describing which generator supplies which bus, and the load sharing between the generators connected to the same bus.
$\boldsymbol{\tau_c}$	Requested generalized forces from the DP-controller. $\boldsymbol{\tau_c} = \begin{pmatrix}F_{surge} & F_{sway} & M_{yaw}\end{pmatrix}^T$.
$f(\cdot)$	User defined function relating cost to produced thrust, consumed power by the thrusters, consumed fuel by the generators, load variations on the bus etc.
T_i	Thrust produced by thruster number i
$T_{i,prev}$	Thrust produced by thruster number i from the previous time-step
p_{T_i}	Power consumed by thruster number i
$p_{T_i}^Q$	Quadratic approximation of the power consumed by thruster number i
p_{G_k}	Power generated by generator number k
$p_{G_k}^Q$	Power generated by generator number k expressed quadratically in the decision variables $\mathbf{u}$.
q_{G_k}	Fuel rate by generator number k
$q_{G_k}^Q$	Fuel rate by generator number k expressed as a quadratic function of the thrusters forces $\mathbf{u}$.
$p_{bus_j}^{avail}$	Total available power on bus number j.
p_{ext_j}	Power consumed by external consumers other than the thrusters.
n	Number of thrusters.
m	Number of buses.
l	Number of generators.
μ_k, ρ_k, γ_i	Scaling factors.

Table 1. Table explaining the notation and symbols used in this paper

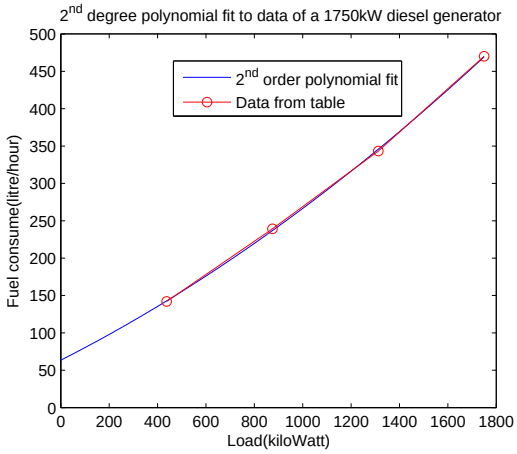

Fig. 1. This figure shows (2) fitted to the data from DieselServiceAndSupply [2013] of a diesel generator rated to $1750kW$

2.1 Static fuel consumption model

The model for the fuel consumption of a generator as a function of its produced power is found by fitting a polynomial of degree 2 to the data given by the table in DieselServiceAndSupply [2013]. This gives us the model shown in (2)

$$q_{G_k} = h_k(p_{G_k}) = a_2 p_{G_k}^2 + a_1 p_{G_k} + a_0 \tag{2}$$

where a_2,a_1 and a_0 are found by fitting the polynomial to the data, and their values will depend on the size of the generator the polynomial is chosen to fit. Fig.1 shows (2) fitted to the data of a diesel generator rated to $1750kW$.

2.2 Defining the cost function

Assuming symmetric load sharing of the generators on each bus we can set up the following set of linear equations.

$$\mathbf{E}\boldsymbol{p_G} = \begin{pmatrix} \boldsymbol{p_{bus}} \\ \mathbf{0}_{(l-m)\times 1} \end{pmatrix} \tag{3}$$

We know that the load on bus number j is given by $p_{bus_j} = \sum_{i=1}^{n} \mathbf{M}_{ji} p_{T_i} + p_{ext_j}$, and by using this together with (3) we can set up the load generated by generator number k as shown in (4).

$$p_{G_k} = \sum_{j=1}^{m}\sum_{i=1}^{n} (\mathbf{E}^{-1})_{kj} \mathbf{M}_{ji} p_{T_i} + p_{ext_j} \tag{4}$$

We notice now that if we chose $f(\cdot)$ to be linear in the fuel consumption, linearise (2) wtr to p_G, make p_G linear in p_T and p_T quadratic in $u_{i,surge}$ and $u_{i,sway}$, $f(\cdot)$ will be quadratic in the decision variables ($u_{i,surge}$ and $u_{i,sway}$).

From Fossen [2002] we know that the power consumed by thruster number i is given by $p_{T_i} = T_i^{3/2}$ and $T_i = \sqrt{u_{i,surge}^2 + u_{i,sway}^2}$, which is obviously not quadratic in the decision variables ($u_{i,surge}$ and $u_{i,sway}$). Several quadratic approximation of this expression are used in the literature e.g Ruth [2008] and Johansen et al. [2004]. In this paper the approximation derived in Ruth [2008] will be used.

$$p_{T_i} \approx p_{T_i}^Q = \frac{T_i^2}{\sqrt{|T_{i,prev}|}} \tag{5}$$

Inserting (5) into (4) gives

$$\begin{aligned} p_{G_k} \approx p_{G_k}^Q &= \sum_{j=1}^{m}\sum_{i=1}^{n} (\mathbf{E}^{-1})_{kj} \mathbf{M}_{ji} p_{T_i}^Q + p_{ext_j} \\ &= \sum_{j=1}^{m}\sum_{i=1}^{n} (\mathbf{E}^{-1})_{kj} \mathbf{M}_{ji} \frac{u_{i,surge}^2 + u_{i,sway}^2}{\sqrt{|T_{i,prev}|}} + p_{ext_j} \end{aligned} \tag{6}$$

Equation (6) now describes the power produced by generator number k expressed quadratically in the decision variables ($u_{i,surge}$ and $u_{i,sway}$).

Linearising (2) wtr to load, around the produced power from the previous time-step using first-order Taylor expansion gives

$$q_{G_k} \approx q_{G_k}^Q = h_k(p_{G_k,prev}) + \frac{dh_k}{dp_{G_k}}(p_{G_k,prev}) \cdot (p_{G_k} - p_{G_k,prev}) \tag{7}$$

where it is chosen to use the superscript ^{Q} to indicate that the fuel consumption is quadratic in the decision variables after the linearization.

We can now use (7) to set up $f(\cdot)$ as a linear function of the fuel consumption, namely $f(q_{G_k}^Q)$ as shown in (8).

$$f(q_{G_k}^Q) = \sum_{k=1}^{l} \frac{1}{\mu_k} q_{G_k}^Q \tag{8}$$

This function is used when solving problem (1) to generate most of the results in this paper. Combining (6)-(7), the cost is quadratic in $\mathbf{u}$.

3. RESULTS

The dynamics of the vessel will not be considered, and it is assumed that as long as the DP-command $\boldsymbol{\tau_c}$ is obtained by the thrust allocation algorithm, the vessel will maintain its position and heading reference Fossen [2002]. Even though the vessel dynamics are not considered, the thruster-/generator- and busbar layout of the vessel are needed. The dimensions for the relevant equipment are also needed in order to get simulations with realistic values. In this paper the specification for the DP class 2 PSV Bourbon Tampen will be used. The specifications of interest are: One $883kW$ tunnel thrusters fwd, one $883kW$ azimuth thruster fwd, two $2500kW$ azipull thrusters aft, two busbars and four $1825kW$ diesel generators. We assume that the vessel operate with open bus-bar.

All the simulations shown in this paper are done over 200 seconds, and the thrust allocation algorithm is executed one time pr second.

In order to save space, the plot that shows that the thrust allocation algorithm obtains the DP-command $\boldsymbol{\tau_c}$ have not been included, however the numerical values are given in kiloNewton(kN).

3.1 Minimizing power vs Minimizing fuel

In this subsection, the problem (1) with (9) as the objective function is compared to the problem (1) with (10) as the objective function with a handful of simulations.

$$J_1 = \mathbf{s}^T \mathbf{Q} \mathbf{s} + \sum_{k=1}^{l} \frac{1}{\mu_k} q_{G_k}^Q \tag{9}$$

$$J_2 = \mathbf{s}^T \mathbf{Q} \mathbf{s} + \sum_{i=1}^{n} \frac{1}{\gamma_i} p_{T_i}^Q \tag{10}$$

J_1 is the objective function in the fuel minimizing problem, while J_2 is the objective function in the power minimizing problem.

In all the simulations, the second term in J_1 that puts a penalty on the use of fuel, is scaled such that it gives a cost between 0-100.

The second term in J_2 that puts a penalty on the power consumed by the thrusters is simulated with two different methods of scaling. One method scales the term such that the thrusters are penalised by a percentage of their total power consumption. The the second method penalises the thrusters equally in the amount of power they consume. In the simulations the second term in J_2 is also scaled such that it returns values between 0-100.

We notice from the results shown in Fig. 2 that the fuel consumption is reduced and that the sum of power consumed by thrusters gets smaller. At first glance this might seem odd, since power was minimized the first 100 seconds! However, because of the scaling of the second term in J_2, the total sum of consumed power by the thrusters is not what is minimized. The scaling of the second term in J_2 used in this simulation prefers the thrusters to consume percentage-wise equal amounts of power. This can be seen in the top-right plot of Fig. 2 where in the first 100 seconds the thrusters work more equally, whereas in the last 100 seconds they separate more. The comparison of the fuel minimizing objective function, with the power minimizing objective function that has this kind of scaling is included in this paper, because it appears to be a common way to scale the second term in J_2.

If we change the scaling of the second term in J_2 such that the sum of total consumed power is minimized, we get the result shown in Fig. 3. Not surprisingly, both the fuel consumption of the generators and power consumption of the thrusters stay almost constant throughout the simulation. We notice that the fuel consumption of each generator, and the power consumption by each thruster changes slightly when the objective function changes. This does have an effect on the total fuel consumption, but it is so small that it cannot be seen in this plot. From the results shown in Fig. 3 one might think that if one minimizes the sum of consumed power by all the thrusters, the fuel consumption will be minimized as well. This however, may not be the case if there are non-zero external load on the buses.

In Fig. 4 both the fuel consumption and power consumed by the thrusters are reduced after the objective function switch. In Fig. 5 however, we notice that the fuel consumption goes down as expected, but the total power consumed

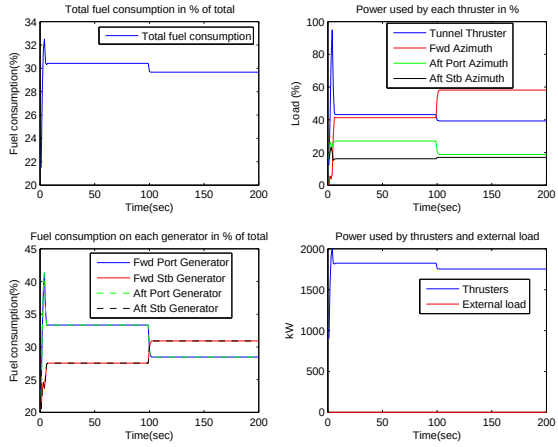

Fig. 2. This simulation is done with $\boldsymbol{\tau_c} = (100\ 200\ 0)^T$ and zero external load. Power consumed by the thrusters is minimized in the first 100 seconds while the last 100 seconds fuel consumption by the generators is minimized. In the first 100 seconds, power consumed by thruster number j is scaled with the inverse of its maximum possible power consumption. $\sim 1\%$ fuel consumption reduction.

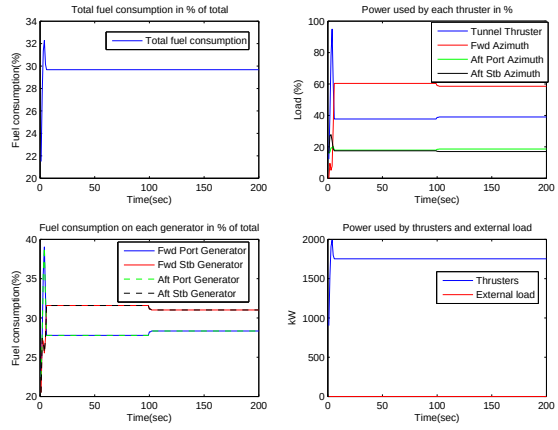

Fig. 3. This simulation is done with $\boldsymbol{\tau_c} = (100\ 200\ 0)^T$ and zero external load. Power consumed by the thrusters is minimized in the first 100 seconds while the last 100 seconds fuel consumption by the generators is minimized. In the first 100 seconds, the power consumption by each thruster is scaled independently of its size. $\sim 0\%$ fuel consumption reduction.

by the thrusters actually increases. This is because of the external load that is present on the port bus bar and the non-linear relationship between thrust, power and fuel. The non-linear relationship between fuel consumption and power production of a generator dictates that the generator gets more efficient at high loads which can be seen from Fig. 1.

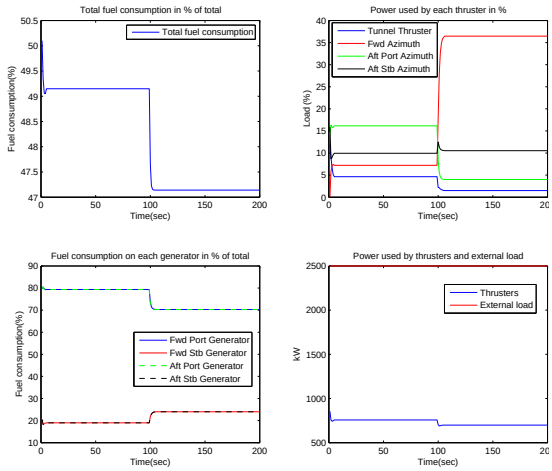

Fig. 4. This simulation is done with $\boldsymbol{\tau_c} = (100\ 50\ 0)^T$ external load of 2500kW on the port bus bar. Power consumed by the thrusters is minimized in the first 100 seconds while in the last 100 seconds fuel consumption, by the generators is minimized. In the first 100 seconds, power consumed by thruster number j is penalised with the inverse of its maximum possible power consumption. $\sim 2\%$ fuel consumption reduction.

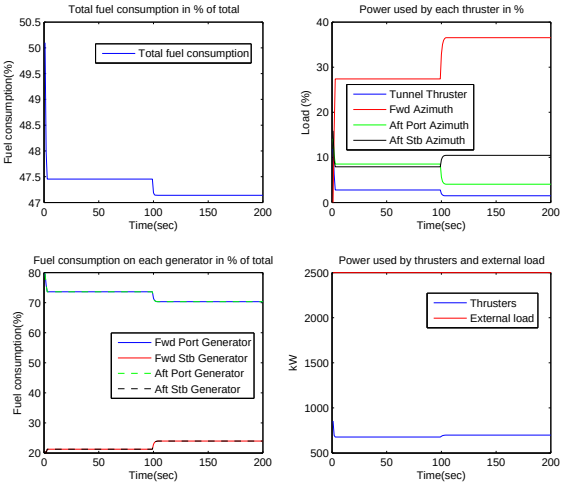

Fig. 5. This simulation is done with $\boldsymbol{\tau_c} = (100\ 50\ 0)^T$ external load of 2500kW on the port bus bar. Power consumed by the thrusters is minimized in the first 100 seconds while the last 100 seconds fuel consumption by the generators is minimized. In the first 100 seconds, the power consumption by each thruster is scaled independently of its size. $\sim 0.5\%$ fuel consumption reduction.

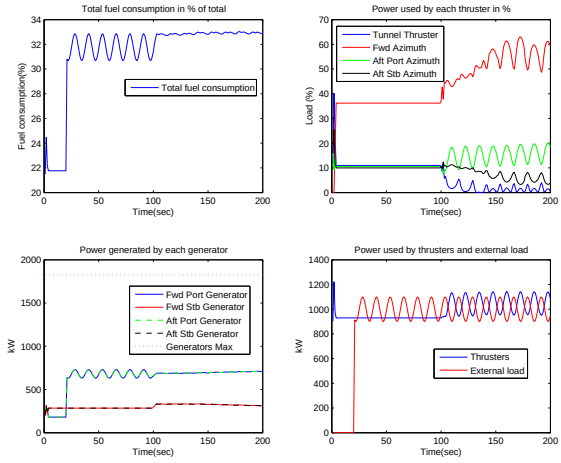

Fig. 6. This simulation is done with $\boldsymbol{\tau_c} = (100\ 100\ 0)^T$ and after 20 seconds an external load on the port bus bar that varies periodically around 1000kW with amplitude of 100kW and a frequency of 0.08Hz is switched on. The first 100 seconds of this simulation minimizes power consumed by the thrusters. After 100 seconds the objective function is switched to (11) which penalises changes in the load on each generator from one time-step to the next.

3.2 Reducing load variations on the generators

In this section simulations of problem (1) with (11) as the objective function are considered.

$$J_3 = \mathbf{s}^T\mathbf{Q}\mathbf{s} + \sum_{k=1}^{l} \frac{1}{\rho_k}\dot{p}_{G_k} + \sum_{k=1}^{l} \frac{1}{\mu_k} q^Q_{G_k} \qquad (11)$$

The 2_{nd} term in J_3 penalizes variations in power produced by the diesel-generators, and the 3_{rd} term in J_3 is included such that fuel is minimized when there are no load variations present on the busbar.

In Fig. 6 we see that thrusters operate at a steady state, while the load on the generators oscillate proportionally to the external load variations for the first 100 seconds. After the objective function switch, we notice that the thrusters starts counteracting the varying external load on the bus, such that the generated load by the generators evens out.

Reducing the load variations will lead to less wear and tear on the generators, and will cause less frequency variations on the bus, which if large enough, can cause a black out. The trade off however, is that the wear and tear on the thrusters will increase which becomes evident by looking at the power consumed by the thrusters in Fig. 6.

How the fuel consumption behaves during the simulation can be seen in the top-left plot of Fig. 6. Since the fuel consumption is based on a static model, the fuel consumption in situations where the dynamics of the diesel generator is excited will not be correctly represented by the model in this paper. The model is a good approximation for the fuel consumption in steady-state situations, or

situations where the load varies slowly enough to not excite the dynamics and large transients on the generator. Hence the real fuel consumption may actually be larger during the first 100 seconds.

In the bottom-left plot of Fig. 6 we notice that the generators connected to the bus with the oscillating external load also has oscillations in their load before the load variation reduction is switched on, which is expected. After the load variation reduction is switched on, the oscillation on these generators are reduced significantly, while the load on the two other generators increase. This means that the mean power produced by the generators are higher after the load variation reduction is switched on. Variations in the power produced by a generator may lead to incomplete combustion which implies higher fuel consumption and more soot pollution. Also, the higher the mean load of the generators are, the more NO_x will be produced. So before the load variation reduction is switched on, the fuel consumption and soot formation will be high, while NO_x production will be low. After the load variation reduction is switched on however, the generators will operate with smaller load variations which implies lower fuel consumption and soot production, but since the mean load increases, then the NO_x production will go up as well. According to Realfsen [2009], the generators has to work above a specific percentage of their maximum capacity in order for cleaning of NO_x to be done by a Selective Catalytic Reduction (SCR)-filter. One might find oneself in a situation then, where by reducing the load variations on the bus and increasing the mean load such that NO_x cleaning can be done, one will effectively reduce wear, fuel consumption, sooting and NO_x emission.

4. CONCLUSION

The fuel optimization can be implemented within the conventional framework of quadratic programming-based thrust allocation, by recalculating the cost function and constraints based on linear and quadratic model approximations at the current operation point.

The fuel minimizing thrust allocation have found solutions that uses less fuel than the power minimizing thrust allocation, except in special situations where there are no external loads. If there are no external load, the fuel minimizing thrust allocation and the power minimizing thrust allocation will produce solutions that will make the generators consume the same amount of fuel. One could say that the fuel minimizing thrust allocation finds solutions that consumes less or equal amounts of fuel as the power minimizing thrust allocation.

When it comes to the load variation reduction, it becomes a trade-off between two things. Not reducing load variations leads to wear and tear on the generators, higher fuel consumption and more sooting. Reducing the load variations will lead to more wear and tear on the thrusters and higher NO_x emission.

REFERENCES

SM Aithal. Modeling of NOx formation in diesel engines using finite-rate chemical kinetics. *Applied Energy*, 87 (7):2256–2265, 2010.

DieselServiceAndSupply. Approximate fuel consumption chart. `http://www.dieselserviceandsupply.com/temp/Fuel_Consumption_Chart.pdf`, 2013.

Thor I Fossen. *Marine Control Systems*. Marine Cybernetics, 2002.

T.I. Fossen and T.A. Johansen. A survey of control allocation methods for ships and underwater vehicles. In *Control and Automation, 2006. MED '06. 14th Mediterranean Conference on*, pages 1–6, 2006. doi: 10.1109/MED.2006.328749.

Lino Guzzella and Christopher H Onder. *Introduction to modeling and control of internal combustion engine systems*. Springer, 2010.

Jan Fredrik Hansen. Modeling and control of marine power systems. *Doctor thesis, Norwegian University of Science and Technology, Department of Engineering cybernetics, Trondheim, Norway*, 2000.

Nils Albert Jenssen and Bjørnar Realfsen. *Power Optimal Thruster Allocation*. MTS Dynamic Positioning Conference, Houston, October 2006.

T.A. Johansen, T.I. Fossen, and S.P. Berge. Constrained nonlinear control allocation with singularity avoidance using sequential quadratic programming. *Control Systems Technology, IEEE Transactions on*, 12(1):211–216, 2004.

Tor A Johansen and Thor I Fossen. Control allocation-a survey. *Automatica*, 49:1087–1103, 2013.

Kjell Erik Larsen. *Fuel-Efficient Control Allocation for Supply Vessels*. Norwegian University of Science and Technology, June 2012. M.Sc Thesis.

John Leavitt. Optimal thrust allocation in dp systems. Houston, 2008. L-3 Communications DPCS, MTS Dynamic Positioning Conference.

Eirik Mathiesen, Bjørnar Realfsen, and Morten Breivik. *Methods for Reducing Frequency and Voltage Variations on DP Vessels*. MTS Dynamic Positioning Conference, Houston, October 2012.

Damir Radan. *Integrated control of marine electrical power systems*. PhD thesis, Norwegian University of Science and Technology, 2008.

Bjørnar Realfsen. *Reducing NOx Emission in DP2 and DP3 Operations*. MTS Dynamic Positioning Conference, Houston, 2009.

Eivind Ruth. *Propulsion control and thrust allocation on marine vessels*. Norwegian University of Science and Technology, 2008. Doctoral Thesis.

Aleksander Veksler, Tor Arne Johansen, and Roger Skjetne. *Transient power control in dynamic positioning - governor feedforward and dynamic thrust allocation*. IFAC Conference on Manoeuvring and Control of Marine Craft, Arenzo, July 2012a.

Aleksander Veksler, Tor Arne Johansen, and Roger Skjetne. Thrust allocation with power management functionality on dynamically positioned vessels. In *American Control Conference (ACC), 2012*, pages 1468–1475. IEEE, 2012b.

Anders Widd. *Physical Modeling and Control of Low Temperature Combustion in Engines*. PhD thesis, Department of Automatic Control, Lund University, Sweden, April 2012.

Christiaan De Wit. *Optimal Thrust Allocation Methods for Dynamic Positioning of Ships*. Delft University of Technology, Netherlands, July 2009. M.Sc Thesis.

APPENDIX B

Bourbon Tampen Technical Specification

TECHNICAL SPECIFICATION

Bourbon Tampen

Platform Supply Vessel

UT 745 E

Revision: 15.02.2006
IMO no: 9276896
DNV id no: 23717
MMSI: 258252000
Call Sign: LLZA

MAIN DESCRIPTION		MEASUREMENT	
Type:	UT 745 E	Lenght oa:	88.60 m
Classification:	DnV + 1A1, SF LFL* COMF-V(3)C(3), E0 DYNPOS-AUTR, CLEAN DK(+) HL(2.5)	Lenght bpp:	78,80 m
		Breath moulded:	18.80 m
Yard:	Kleven Verft AS	Depth moulded:	7.60 m
Yard built no:	295	Draught max:	6,20 m at 4350 tns
Place built:	Ulsteinvik	Gross tonnage GT:	3325 t
Country built:	Norway	Corresponding DWT:	3500 t
Delivered:	2002	Net tonnage NT:	1366 t
Flag:	NOR		
Port of registry:	Fosnavåg		
Owner:	Bourbon Ships AS	ISM-Responsible:	Bourbon Offshore Norway AS

CARGO CAPACITY		DISCHARGE RATES	
Deck cargo:	2800 t	Loading/Discharge station:	Each sides 4-5" weco connection
Deck area:	990 m², with cargo barrier fwd.	Fuel discharge rate:	2 x 250 m³/hour, 9 bar, Hydr.driven
Deck strength:	10,0 t/m²	Mud discharge rate:	4 x 100 m³/hour, 24 bar, Hydr.driven
Fuel (gasoil):	1337 m³	Brine discharge rate:	2 x 100 m³/hour, 24 bar, Hydr.driven
Liquid Mud:	600 m³	Drillwater discharge rate:	2 x 250 m³/hour, 9 bar, Hydr.driven
Brine:	400 m³	Dry Bulk discharge rate:	2 x 23 m³/min, 5,6 bar
Drillwater/Ballast:	862 m³	Base Oil discharge rate:	2 x 150 m³/hour, 15 bar, Hydr.driven
Base Oil:	294 m³	Fresh Water discharge rate:	2 x 250 m³/hour, 9,0 bar, Hydr.driven
Dry Bulk:	400 m³	Methanol discharge rate:	2 x 100 m³/hour, 9 bar, Hydr.driven
Fresh Water:	734 m³	Slop discharge rate:	2 x 150 m³/hour, 9 bar, Hydr.driven
Methanol:	160 m³		
Slop:	313 m³		

MACHINERY / PROPULSION

Main Engine set 1:	2 x Caterpillar 3516 TA 1825 kW-1800RPM	Bow Thruster 1:	1 x RRM 250 TV- SS 1200 RPM, 883 kW
Main Engine set 2:	2 x Caterpillar 3516 TA 1825 kW-1800RPM	Compass Thruster Forward:	R&R, TCNS 73/50-180, 304 rpm 883 kW
Propulsion Aft:	2 x Rolls & Royce Azipull Thrusters 2500 kW	Main Generators set 1:	2 x ABB, Merlin Gerin NW-25 HA, 2281 KVA
Total BHP:	9928 BHP	Main Generators set 2:	2 x ABB, Merlin Gerin NW-25 HA, 2281 KVA
Total Kw:	7300 kW	Emergency Generator:	1 x Caterpillar 3408 TA ,385 kW
		Shore Connection:	440 V- 200A